



HAL
open science

Development of a novel target-based cell assay, reporter of the activity of Mycobacterium tuberculosis protein- O-mannosyltransferase

Nicolas Géraud, Camille Falcou, Julien Parra, Carine Froment, David Rengel, Odile Burette-Schiltz, Julien Marcoux, Jérôme Nigou, Michel Rivière, Emeline Fabre

► To cite this version:

Nicolas Géraud, Camille Falcou, Julien Parra, Carine Froment, David Rengel, et al.. Development of a novel target-based cell assay, reporter of the activity of Mycobacterium tuberculosis protein- O-mannosyltransferase. *Glycobiology*, 2023, 10.1093/glycob/cwad072 . hal-04264267

HAL Id: hal-04264267

<https://hal.science/hal-04264267v1>

Submitted on 3 Nov 2023

HAL is a multi-disciplinary open access archive for the deposit and dissemination of scientific research documents, whether they are published or not. The documents may come from teaching and research institutions in France or abroad, or from public or private research centers.

L'archive ouverte pluridisciplinaire **HAL**, est destinée au dépôt et à la diffusion de documents scientifiques de niveau recherche, publiés ou non, émanant des établissements d'enseignement et de recherche français ou étrangers, des laboratoires publics ou privés.

25 **ABSTRACT**

26

27 The Protein-*O*-mannosyltransferase is crucial for the virulence of *Mycobacterium tuberculosis*, the
28 etiological agent of tuberculosis. This enzyme, called MtPMT (Rv1002c), is responsible for the post-
29 translational *O*-mannosylation of mycobacterial proteins. It catalyzes the transfer of a single mannose
30 residue from a polyprenol phospho-mannosyl lipidic donor to the hydroxyl groups of selected Ser/Thr
31 residues in acceptor proteins during their translocation across the membrane. Previously, we provided
32 evidence that the loss of MtPMT activity causes the absence of mannoproteins in *Mycobacterium*
33 *tuberculosis*, severely impacting its intracellular growth, as well as a strong attenuation of its
34 pathogenicity in immunocompromised mice. Therefore, it is of interest to develop specific inhibitors
35 of this enzyme to better understand mycobacterial infectious diseases. Here we report the
36 development of a "target-based" phenotypic assay for this enzyme, assessing its *O*-
37 mannosyltransferase activity *in bacteria*, in the non-pathogenic *Mycobacterium smegmatis* strain.
38 Robustness of the quantitative contribution of this assay was evaluated by intact protein mass
39 spectrometry, using a panel of control strains, overexpressing the MtPMT gene, carrying different key
40 point-mutations. Then, screening of a limited library of 30 compounds rationally chosen allowed us to
41 identify 2 compounds containing pyrrole analogous rings, as significant inhibitors of MtPMT activity,
42 affecting neither the growth of the mycobacterium nor its secretion of mannoproteins. These
43 molecular cores could therefore serve as scaffold for the design of new pharmaceutical agents that
44 could improve treatment of mycobacterial diseases. We report here the implementation of a
45 miniaturized phenotypic activity assay for a glycosyltransferase of the C superfamily.

46

47

48 INTRODUCTION

49 *Mycobacterium tuberculosis* (Mtb) remains the world's deadliest bacterial pathogen in 2020, with
50 nearly 10 million newly infected people and 1.5 million deaths due to tuberculosis (TB), including
51 214,000 HIV-positive people (WHO, 2021). Moreover, contrasting with the steady decline of the
52 disease burden resulting from decades of global efforts and commitments, we are currently witnessing
53 an alarming annual 10% increase in the number of cases of antimicrobial-resistant (AMR) TB. This
54 threat unveils the risk of shortage in our effective anti-tuberculosis therapeutic arsenal and urges the
55 research and development for new treatments to prevent future out-of-control epidemics of drug-
56 resistant TB. A reason for this setback is the strong selection pressure maintained by protracted and
57 burdensome anti-tuberculosis treatments targeting essential physiological processes and hence
58 promoting the emergence of AMR bugs. Therefore, several “non-traditional” antimicrobial therapeutic
59 strategies are currently explored to circumvent this drawback associated with classical antibiotics,
60 including the very appealing anti-virulence approach that aims at targeting pathways not essential in
61 *in vitro* culture but indispensable for host colonization and/or infection (Clatworthy et al., 2007;
62 Theuretzbacher and Piddock, 2019; Rex et al., 2019; Gigante et al., 2022).

63 In this regard, we previously reported that secreted *O*-mannosylated proteins are not essential for Mtb
64 growth in laboratory conditions, but crucial for adhesion to host cells, intracellular survival and Mtb
65 virulence in a rodent animal model (Ragas et al., 2007; Liu et al., 2013). To date, more than sixty *O*-
66 mannosylated proteins secreted by Mtb have been identified from standard laboratory cultures, many
67 of which are important effectors contributing to the *bacilli* defenses against the host immune response
68 (Tonini et al., 2020). These mannoproteins (*such as* Apa/Rv1860, MPB/T83/Rv2873, LpqH/Rv3763,
69 SodC/Rv0432 or PstS-1/Rv0934) can modulate the inflammatory response, in particular by interacting
70 with lectin receptors on macrophages, allowing bacteria to enter and survive longer in these cells
71 (Pitarque et al., 2005; Ragas et al., 2007; Schnappinger et al., 2003; Stewart et al., 2005; Sartain and
72 Belisle, 2009; Esparza et al., 2015; Torrelles and Schlesinger, 2010).

73 Although the relevance of the mannoprotein mannosyl appendages has never been clearly and
74 definitively confirmed as decisive for the biological activity of any of these glycosylated proteins
75 (Alonso et al., 2017), as a whole, the mannoproteome meets the definition of non-essential virulence
76 factor by contributing to the infectiousness and pathogenicity of the *bacilli*.

77 To date, protein-*O*-mannosylation is the only protein glycosyl post-translational modification
78 demonstrated formally in *Mtb* and is initiated by the Protein-*O*-Mannosyltransferase MtPMT encoded
79 by the Rv1002c gene. This enzyme catalyzes the transfer of single mannose units from polyprenol
80 phospho-mannosyl lipidic donors to the hydroxyl groups of selected threonines or serines (S/T) of
81 acceptor proteins during their translocation across the membrane. These initial single mannosyl
82 entries are then generally progressively elongated through successive addition of mannosyl units by
83 the (α 1 \rightarrow 2) mannosyl transferase PimE (Rv1159) (Liu et al., 2013) to form linear manno-
84 oligosaccharides containing up to 8 residues (Parra et al., 2017) (**Fig. 1A, B and C**). This process
85 generates substantial repertoires of proteoglycoforms differing by the total number of mannosyl
86 residues but also the length and position of the different manno oligosaccharides, as previously
87 illustrated by the mass spectrometry analysis of the P₂₇₋₅₁ mannosylated peptide from LpqH (**Fig. 1C**)
88 (Parra et al., 2017). Since these different proteoglycoforms may differ in their biological activity, the
89 whole blockade of the protein-*O*-mannosylation process by chemical inhibition of the sole protein
90 mannosylating enzyme MtPMT would constitute a valuable non-traditional alternative to abrogate
91 *Mtb* virulence *in-vivo* (van Els et al., 2014; Mehaffy et al., 2019). PMTs are polytopic membrane
92 proteins belonging to the GT-C glycosyl transferase family to which also belongs the mycobacterial
93 arabinosyl transferase EmbA, target of the first line antituberculous drug ethambutol. However, unlike
94 EmbA, there is no known specific inhibitor for MtPMT. Moreover, the only PMT inhibitor reported to
95 date is selective of the eukaryotic PMT-1 isotype family (Orchard et al., 2004). In addition, the complete
96 lack of knowledge concerning the mode of action of this compound, as well as the limited knowledge
97 of the GT-C family enzyme, preclude any attempt for a rational discovery of potential MtPMT inhibitor
98 candidates from this initial lead. As an alternative, high-throughput screening (HTS) remains the

99 method of choice to discover potential MtPMT inhibitors without *a priori*. However, this blind
100 approach often remains challenging, particularly for glycosyltransferases such as PMTs that are not
101 easily amenable to HTS approaches (Chao and Jongkees, 2019). Indeed, a major obstacle is the
102 difficulty to read out the transfer of mannose residues on target proteins. This has been assessed by
103 different approaches, including monitoring the transfer of radiolabeled mannose onto an acceptor
104 peptide (Schultz and Takayama, 1975; Cooper et al., 2002), detecting protein glycosylation by western
105 blotting using mannose binding concanavalin A lectin (ConA) (Garbe et al., 1993), assessing
106 mannosylation-induced protein apparent-mass-increase by gel electrophoretic mobility delay
107 (Girrbach et al., 2000), or characterizing peptide glycosylation by mass spectrometry (Dobos et al.,
108 1995; VanderVen et al., 2005; Smith et al., 2014; Tonini et al., 2020). Although efficient, most of these
109 approaches are poorly quantitative and rather cumbersome due to multiple sample handlings that are
110 poorly compatible with HTS robotic platforms.

111 The second major hurdle comes from the membrane-embedded intrinsic nature of MtPMT, that makes
112 the mannose transfer activity depend on a complex lipidic surrounding. Indeed, this environment
113 ensures the spatial colocalization of the MtPMT polytopic enzyme with both the mannose donor
114 embedded in the lipid bilayer, and the acceptor polypeptide chain being translocated into the
115 periplasm by the SecYEG translocon (Loibl et al., 2014). The difficulty to reconstitute to functionality
116 of such a system from its isolated components or to control the relative concentrations of its different
117 constituents within a bacterial crude lysate or membrane extract, strongly hampers the development
118 of a robust cell-free assay amenable to high throughput (Cooper et al., 2002). These shortcomings are
119 generally circumvented by cell-based inhibitor screening assays, which in addition allow assessing
120 transport and bioavailability of the candidate effector, limiting the severe attrition typically seen with
121 candidates issued from cell-free assays (Clatworthy et al., 2007; Gigante et al., 2022). However, these
122 so-called “phenotypic” approaches are typically non-target specific, and the growth-inhibitory activity
123 (live-dead bacteria) on which they are commonly based does not apply to MtPMT, as by definition it is

124 non-essential and its arrest does not affect growth or kill Mtb under laboratory conditions
125 (Theuretzbacher and Piddock, 2019).

126 Nonetheless, in view of the potential therapeutic relevance of the pleiotropic interruption of protein-
127 *O*-mannosylation, we focused our efforts on the development of a down-sizable MtPMT activity assay,
128 compatible with medium to high throughput screening of chemicals able to inhibit *in cellulo* the
129 mannosylation by MtPMT of mycobacterial-secreted proteins.

130 With this aim, and to circumvent the stringent and burdensome cultivation conditions of Mtb, MtPMT
131 was expressed ectopically in the nonpathogenic fast-growing *Mycobacterium smegmatis* (*M.*
132 *smegmatis*) invalidated for its own MsPMT. The resulting recombinant strain was modified further to
133 over-express the poly-histidine tagged secreted protein Fasciclin (FasC^{His}) as a substrate acceptor of
134 MtPMT. The biological function of the fasciclin domains present in some mycobacterial proteins (FasC
135 from *M. smegmatis* ; MPT83/Rv2873 and MPT70/Rv2871 from Mtb) remains unclear. However, on the
136 basis of structural homology with human fasciclin, it has been proposed that these domains are
137 involved in cell adhesion (Carr et al., 2003; Wiker, 2009). Functionality and workability of the reporter
138 strain were assessed by conventional characterization of mannosylation of the secreted FasC^{His} and
139 the level of ConA binding to the affinity-purified FasC^{His} was validated as a surrogate value for
140 quantification of the MtPMT activity. Reporter strain cultivation, FasC purification and ConA binding
141 quantification steps were further optimized and downsized to be performed in 96-well microtiter plate
142 format. As a proof of concept, validation of this automation compatible MtPMT activity cell-based
143 assay was achieved by mid-throughput scanning of a preliminary library of about thirty rationally
144 chosen compounds. This reporter strategy constitutes an example of a target-based cell assay to
145 monitor the activity *in cellulo* of a non-essential polytopic bacterial membrane enzyme involved in the
146 post-translational modifications of secreted proteins.

147

148 **RESULTS**

149 **Construction of a mycobacterial MtPMT activity reporter strain**

150 To develop a readily workable cellular assay to monitor the *in situ* activity of MtPMT, we generated an
151 appropriate surrogate reporter strain to overcome the restrictive safety and time constraints raised by
152 cultivation of the pathogenic and slow growing Mtb. With this aim, we chose to use as starting material
153 the non-pathogenic *M. smegmatis* mc²155 for its rapid growth phenotype, its genetic proximity to Mtb
154 and its natural capacity to produce and secrete mannoproteins. As a preliminary step, the *M.*
155 *smegmatis* endogenous protein-*O*-mannosylating enzyme coded by the MSMEG_5447 was disrupted
156 by allelic exchange, to generate the recombinant recipient strain named (Msm-Δ(MsPMT)) (**Fig. 2**) (Liu
157 et al., 2013). This mannoprotein-defective strain was transformed in turn with an episomal vector
158 bearing the Mtb Rv1002c gene under the control of the mycobacterial pBlaF* promotor (Spratt et al.,
159 2003) allowing constitutive ectopic expression of MtPMT in *M. smegmatis* (Lee and Hatfull, 1993).
160 Notably, the two amino acid sequences of MtPMT and MsPMT share 93% similarity and 75% identity.
161 Finally, the latter recombinant strain (Msm-ΔMsPMT::MtPMT) was further modified with a multicopy
162 replicative plasmid harboring the MSMEG_5196 gene fused to the hexa-histidine coding sequence, to
163 over-express constitutively an easy-to-detect secreted acceptor substrate of MtPMT: the FasC^{His}. This
164 naturally secreted mannoprotein of *M. smegmatis* was chosen because of its high abundance in the
165 culture medium and high degree of mannosylation (up to 13 hexoses), which makes it a sensitive probe
166 of the MtPMT mannosyl transfer activity (Liu et al., 2013) (**Fig. 1 and 2**). Thanks to this, the ectopic
167 expression and heterologous activity of MtPMT in *M. smegmatis* can be verified by analysis of the
168 glycosylation pattern of the NiNTA-purified FasC^{His} secreted by the recombinant reporter strain (Msm-
169 ΔMsPMT::MtPMT).

170 As shown by SDS-PAGE revealed by Coomassie blue staining or by Western blot with an anti-HisTag
171 mAb (**Fig. 3A**), FasC^{His} purified from the culture medium of the recipient strain (Msm-ΔMsPMT, called
172 no-PMT) transformed with the empty vector and defective for protein mannosylation appears as a thin
173 band as expected for this non-glycosylated control. In contrast, FasC^{His} purified from the reporter strain

174 (Msm- Δ MSPMT::MtPMT, called WT) exhibits a broader band profile consistent with mass dispersion
175 induced by multiple and heterogeneous glycosylation.

176 Further accurate inspection by Liquid Chromatography-Electro Spray Ionisation Mass Spectrometry
177 (LC-ESI-MS) confirms this hypothesis by highlighting the precise differences in molecular weight (MW)
178 profile of the proteins purified from the two strains (**Fig. 3A and Sup. fig. 1**). Indeed, consistent with
179 the protein mannosylation defect of the recipient strain, the deconvoluted mass spectrum of the Fas^{His}
180 purified from the Msm- Δ MSPMT (called no-PMT) strain shows a single peak at 23,845 Da attributable
181 to the non-glycosylated protein (theoretical average MW 23,845 Da). This aglycosylated form of the
182 protein also represents the most intense peak of the mass spectrum of the Fas^{His} purified from the
183 reporter strain Msm- Δ MSPMT::MtPMT (WT). However, in addition to this peak at 23,845 Da, a series
184 of peaks regularly spaced by 162 Da mass shifts indicates the presence of at least 13 Fas^{C^{His}} glycoforms,
185 accounting for almost 80% of the cumulated peak area. This complex mass profile resulting from the
186 accumulative decoration of the protein by oligomannosyl appendages confirms the orthogonal
187 mannosyl transferase activity of Mtb MtPMT in *M. smegmatis*.

188 To verify whether the MS profile of the purified Fas^{C^{His}} could reflect quantitative alteration of the
189 enzymatic activity, we generated several similar reporter strains expressing a single amino acid
190 mutated sequence of MtPMT, L366A, Y371A and Y444A. These mutations, predicted to be located in
191 soluble external loops by sequence homology with the fungal enzymes ScPMT1/2 (Bai et al., 2019),
192 were chosen for their regularly spaced deleterious effects on MtPMT activity. Comparison of the MS
193 profiles of the Fas^{C^{His}} purified from these different mutated strains reveals that the MtPMT substitutive
194 mutations are associated with significant decreases in the number and intensities of the glycosylated
195 form signals relative to those of the unsubstituted protein. Since these differences are solely
196 attributable to the impact of the mutations on the initial mannose transfer by MtPMT onto the
197 acceptor substrate, the Fas^{C^{His}} MS profiles therefore appear as reliable semi-quantitative indicators of
198 the relative activities of the mutated enzymes *in vivo* (**Fig. 3B and C, and Sup. fig. 2**). In conclusion,

199 altogether these results confirm the effectiveness of the reporter cell system to assess the *in situ*
200 activity of MtPMT in *M. smegmatis*.

201 However, the LC-MS workflow requires the pre-analytical purification of the reporter FasC^{His} that is
202 poorly compatible with the search for MtPMT inhibitors in massive chemical libraries.

203 Alternatively, multi-well plate format quantitative enzyme linked lectin assay (ELLA) turned out to be
204 an alternative for quantifying FasC^{His} relative mannosylation, because of its multiplexing capabilities
205 allowing for the simultaneous quantification of multiple samples in a high-throughput manner, such as
206 heterogeneous complex bacterial supernatants.

207 **Development of a miniaturized MtPMT activity phenotypic assay**

208 In order to develop an assay for quantifying FasC^{His} mannosylation directly from crude microculture
209 supernatants, we implemented the detection of Concanavalin A (ConA) binding to FasC^{His}
210 oligomannosides. Adjustment of the assay to the multi-well plate format implies down-scaling the
211 entire workflow, including (1) the culture of reporter cells and production of the MtPMT acceptor
212 substrate FasC^{His}, (2) the isolation of FasC^{His} from the pool of ConA binding manno-conjugates present
213 in the culture supernatant, and (3) the quantification of FasC^{His} mannosylation. Keeping in mind the
214 possibility to transfer the assay to a robotic platform for middle/high-throughput screening for
215 potential MtPMT inhibitors we chose to demonstrate the feasibility based on the 96-well plate format.

216 **Reporter cell culture and FasC^{His} production.** Since protein expression of proteins are highly dependent
217 on bacterial culture conditions, we first monitored the production of secreted FasC^{His} by the reporter
218 strain grown in the reduced volume of the microplate well (250 μ L). Best results were obtained with
219 reporter cells generated extemporaneously, to minimize potential instability of FasC^{His} production that
220 tends to decrease over repeated cultures of the recombinant strain. In brief, newly transformed
221 reporter cells picked up from selective solid medium are expanded once in liquid culture for 7 days
222 before use. Then, the 96-well plates filled with 200 μ L/well of fresh medium are seeded at a final OD₆₀₀
223 0.1 with an aggregate-free cell suspension prepared from the primary liquid culture. Cells are grown

224 for 7 days and the level of FasC^{His} production in the crude cell culture supernatant is monitored over
225 the time course of the culture, either by Coomassie blue stained SDS-PAGE, or by ELISA using anti His-
226 tag antibodies. Both approaches reveal a time dependent increase in FasC^{His} abundance as a result of
227 the accumulation of newly secreted protein in the culture medium. Interestingly, the downscaling of
228 the culture volume from 10 mL flask to 250 μ L microplate wells only marginally affects cell growth
229 ($OD_{600nm} \sim 1$ at day 7). In contrast, quantification by anti His-tag ELISA after 7 days of cultivation shows
230 a slightly higher FasC^{His} concentration close to 200 μ g/mL in microplate reduced volume, compared to
231 cultures in greater volume flasks (**Sup. fig. 3 A and B**). Hence, this reproducible result confirms *in fine*
232 that the production of FasC^{His} by the recombinant reporter strain is only slightly affected by the 40-fold
233 reduction of the culture volume from 10 mL flasks to 250 μ L microplate wells.

234 ***FasC^{His} isolation and mannosylation quantification.*** The relative quantification of FasC^{His}
235 mannosylation by ConA binding requires the preliminary isolation of the FasC^{His} reporter protein from
236 the bulk pool of glycoconjugates present in the culture supernatant, mainly mannophosphoinositides,
237 lipoglycans and polysaccharides that are likely to interact with the lectin. This is readily achieved
238 simultaneously on multiple samples by selective capture of the His-tagged protein using multi-well
239 plates precoated with specific anti-His-tag antibodies. The rate of mannose branching of the proteins
240 captured this way can then be estimated with HRP-conjugated ConA that binds preferentially to
241 terminal mannose residues directly linked to the protein or localized at the non-reducing end of small
242 linear manno-oligosaccharides (**Fig. 4A**). The performances in terms of sensitivity and reliability of the
243 approach for the quantification of FasC^{His} mannosylation, are clearly attested by the relative dose
244 dependent binding of ConA to the FasC^{His} contained in the culture supernatant of reporter strains
245 harboring mutated MtPMT (**Fig. 4B**).

246 The ConA-binding dose-response curve to FasC^{His} from the culture supernatant of the Msm-
247 Δ MSPMT::MtPMT reference strain shows a hyperbolic shape with a likely initial linear dose response
248 (at the highest supernatant dilution) that rapidly reaches a plateau for FasC^{His} concentration above 4

249 ng/ μ L. At the opposite end, the non-glycosylated form of FasC^{His} obtained from the Msm- Δ MSPMT and
250 Msm- Δ MSPMT::MtPMTY444A strains shows ConA binding signals indiscernible from the basal
251 background, as expected from the absence or quasi absence of mannosyl appendages on these
252 molecules. Interestingly, the in-between signal of ConA binding of 80% and 60% observed for the
253 FasC^{His} produced by the recombinant strains harboring mutated MtPMT, Msm- Δ MSPMT::MtPMTL366A
254 and Msm- Δ MSPMT::MtPMTY371A, is fully consistent with their intermediate glycosylation level
255 evidenced by LC-MS analyses (**Fig. 4C**). In addition, the ConA binding curves obtained for these lesser
256 glycosylated forms of FasC^{His} show similar profiles compared to the fully glycosylated FasC^{His}, with a
257 plateau occurring at the same saturating concentration, which corresponds to a quantity of about 200
258 ng of FasC^{His} per well, consistent with the maximum binding capacity range claimed by the
259 manufacturer (150-300 ng of poly-histidine tagged protein/well). Thus, provided one works above this
260 saturating concentration, this intrinsic limitation in the amount of immobilized His-tagged ligand allows
261 convenient normalization of the ConA binding response versus the concentration of FasC^{His} to quantify
262 the protein mannosylation and to assess the mannosyltransferase activity of MtPMT *in vivo*.

263 Finally, a remarkable correlation is observed between the data obtained by ELLA and LC-MS analysis
264 though they differ radically in that the latter approach is performed on purified FasC^{His} only while the
265 former operates directly on crude microculture supernatants. Both quantitations provide similar
266 patterns of protein-*O*-mannosylation attenuation among the different genetic backgrounds
267 (WT>L366A>Y371A>Y444A>No-PMT), and thus confirm the quantitative ELLA as a valid and convenient
268 approach to assess the MtPMT activity *in cellulo*.

269 **Implementation of the mycobacterial MtPMT phenotypic assay**

270 To validate the approach for medium-throughput screening (MDS) of potential protein-*O*-
271 mannosylation inhibitory compounds, a set of 30 chemicals were assessed with this novel target-based
272 cell assay, according to the experimental workflow schematized in **Fig. 5**. These 30 compounds were
273 rationally chosen for their putative inhibitory effect on MtPMT activity, as biomimetics of proline-

274 enriched mycobacterial manno-peptides (Laqueyrie et al., 1995; Smith et al., 2014). Briefly, freshly
275 prepared *M. smegmatis* Msm-ΔMsPMT::MtPMT WT-reporter cells are cultured in duplicate in 96-well
276 microplates in the presence of increasing concentrations (2.5, 25 and 250 µg /mL) of the selected
277 compounds (**Fig. 5A**). After 7 days, the OD_{600nm} are measured and the supernatants are collected to
278 verify the putative effect of the compound on the MtPMT activity by quantification of FasC^{His} relative
279 mannosylation by ConA ELLA (**Fig. 5A and B**). In a first instance, inactive compounds or those inducing
280 growth inhibition are disregarded. Besides, those associated with reproducible and coherent dose-
281 dependent decrease in the level of mannose binding to ConA are considered for additional controls of
282 the FasC^{His} production (**Fig. 5C**). Indeed, the aim of the latter control is to exclude any bias due to a
283 decline in the expression or secretion of the mannosylated FasC^{His} below the saturating concentration
284 required to normalize the responses for comparison.

285 Among the 30 chosen compounds, we first wanted to test several rhodamine derivatives (**Fig. 6A, Table**
286 **II**), including R3A-5a also referenced as OGT2599, previously reported as inhibitor of yeast and mice
287 PMTs (Szafranski-Schneider et al., 2012; Orchard et al., 2004). We also included two rhodamine
288 containing chemicals reported to selectively kill non-replicating MTb (Bryk et al., 2008) in order to
289 verify whether this specific bactericidal activity could be associated with protein-*O*-mannosylation
290 deficiency. Beside this class of substances, we chose to test several pyrrole or pyrrolidine-containing
291 compounds that could present analogies with the proline-rich sequences surrounding the Thr/Ser
292 targeted by the MtPMT (Smith et al., 2014). The rationale here is that this kind of biomimetic may
293 compete with the acceptor substrate for the binding to the enzyme (**Fig. 6A, Table II**).

294 Finally, we blind-tested several molecules without prior knowledge of their structures, including
295 glycosyltransferase transition-state substrate-analogues, or rhodamine derivatives (**Table II**). The
296 effects of each of these 30 chemicals on mycobacterial growth, the FasC^{His} relative-*O*-mannosylation
297 and FasC^{His} secretion were analyzed thoroughly. The results confirm that neither the rhodamine 3-

298 acetic acid derivative R3A-5a (OGT2599) nor the rhodamine-containing chemicals are likely to alter the
299 bacterial MtPMT activity, at these concentrations.

300 Of the 30 compounds tested, 8 show probable FasC^{His} relative mannosylation reduction, among which
301 3 molecules induce a statistically significant dose-dependent inhibitory effect (Z317129322,
302 Z66495095, and D-Proline, see **Fig. 6B** and **Sup. fig. 3**). These 8 compounds all contain pyrrole analogs,
303 and most significantly, with D-Proline, a maximum inhibition of 29±2% was observed with
304 concentrations ranging from 2.5 µM to 250 µM. Interestingly, the two compounds with the highest
305 inhibitory effects on MtPMT activity (compounds Z66495095 and D-Proline) had no effect on either
306 bacterial growth or FasC^{His} secretion (**Fig. 6C and D**), two crucial criteria for avoiding the induction of
307 drug resistance mechanisms. In contrast, OD_{600nm} measurements revealed a dose-dependent inhibitory
308 effect on mycobacterial growth for four compounds (Z280700946, Z5816758, Z269692472, and
309 Z317129322, **Fig. 6C**). However, despite these dose-dependent growth declines, the concentrations of
310 FasC^{His} in the different supernatants were above the maximum capture-capacity of the anti-His-tag
311 antibody-coated well (*i.e.*, more than 200 ng/well, see **Fig. 6D**), confirming that the observed relative
312 ConA binding decrease results from a lower FasC^{His} mannosylation rather than from a diminution of
313 the FasC^{His} concentration.

314 This control validates our interpretation that the decrease in ConA binding (observed for the 8 pyrrole-
315 derived compounds) reflects a lower mannosylation of FasC^{His} glycoforms, attributable to an inhibitory
316 effect exerted on MtPMT activity. Notably, compounds Z5816758, Z269692472, and Z317129322
317 appeared to inhibit FasC^{His} secretion, in a dose-dependent manner (**Fig. 6D**), while neither L-Proline
318 nor pyrrolidine showed any significant inhibitory effect compared to D-Proline under the same test
319 conditions (not shown), suggesting that the stereochemistry and the conformation of these molecules
320 are determinant factors in the inhibition of MtPMT (**Fig. 6A**).

321 Overall, our results demonstrate the operability and reliability of this unique multiplexed target-based
322 cell assay to evidence the eventual MtPMT activity alterations induced by chemicals *in cellulo*. This

323 achievement opens the way for the development of MDS/HTS campaigns to identify specific inhibitors
324 of bacterial PMTs of pharmacologic potential, for the development of non-conventional anti-
325 tuberculous adjuvant therapies.

326 **DISCUSSION**

327 The MtPMT enzyme, encoded by the Rv1002c Mtb gene, is non-essential for the microorganism
328 growth, but crucial for its virulence (Liu et al., 2013). This protein is the only Mtb enzyme that catalyzes
329 the initial transfer of mannoside units onto mannoproteins acting as "acceptor" substrates (VanderVen
330 et al., 2005) and being subsequently either secreted or anchored at the membrane (Tonini et al., 2020).
331 After transfer of the first mannoside units by MtPMT, the oligomannosides are then extended by
332 elongating enzymes in a linear, unbranched fashion (Liu et al., 2013). Therefore, in mycobacteria,
333 measurement of the rate of terminal mannosylation of oligomannosylated-proteins reflects that of
334 initial *O*-mannosylation, *i.e.*, the activity of MtPMT. In the present work, we sought to exploit this
335 relationship to measure MtPMT activity, via the measurement of the binding rate of ConA, a lectin that
336 specifically recognizes terminal mannoside units. Our goal was to initiate the search for MtPMT
337 inhibitors that would be effective in a native biological context. Therefore, we first constructed a
338 reporter strain heterologously producing MtPMT in *M. smegmatis*, a non-pathogenic mycobacterium.
339 Then we developed a high-throughput phenotypic MtPMT activity-assay, based on the detection of
340 ConA binding to FasC, chosen as secreted, highly mannosylated mycobacterial reporter of MtPMT
341 activity. As a proof of concept, we applied our phenotypic assay to the screening of a reduced panel of
342 rationally selected compounds.

343 Remarkably, the catalytic site of PMT enzymes is highly conserved among species, consisting primarily
344 of a triad of essential amino acids, which catalyze the transfer of mannoside units from a glycolipidic
345 substrate, "donor" of mannoside units (Bai et al., 2019). Due to this high conservation, the catalytic
346 site appeared to us unattractive as a specific molecular target for inhibitors of MtPMT activity, which
347 should be free of host toxicity for future therapeutic applications. In contrast, the species-specific

348 donor and acceptor substrate binding sites seemed more relevant to target. Given these
349 pharmacological imperatives, we noticed that the literature on PMTs mentioned the F664S
350 substitution in the PpPMT2 enzyme sequence of the yeast *Pichia pastoris*, as related to strong fungal
351 resistance to rhodamine analogs (Argyros et al., 2013). Together with recent information provided by
352 the resolution of the 3D structures of *Saccharomyces cerevisiae* ScPMT1/2 in complex with their donor
353 and acceptor substrates (Bai et al., 2019), this observation suggested that rhodamine-derived
354 compounds might bind to the enzymatic active sites. Indeed, F664 of PpPMT2 from *Pichia pastoris*
355 align with S644 of ScPMT1 from *S. cerevisiae*, which is in direct contact with the periplasmic extremity
356 of the dolichol carbon chain, and in close proximity with the phosphomannoside unit (Bai et al., 2019).
357 Unfortunately, according to our results, no rhodamine derivatives were found to inhibit MtPMT
358 activity, whereas the compound R3A-5A, in particular, had been reported to inhibit the activities of
359 several yeast PMTs, such as *Candida albicans* (Orchard et al., 2004), *Saccharomyces cerevisiae* (Arroyo
360 et al., 2011), and *Pichia pastoris* (Argyros et al., 2013). These negative results could be explained by
361 the impermeability of the mycobacterial membrane to these highly hydrophobic compounds, or
362 alternatively by the low or no affinity of these molecules for our mycobacterial target enzyme. The
363 latter interpretation therefore encourages further investigations dedicated to the inhibition of
364 glycolipid donor substrate binding, in order to discern the targeting of mycobacterial PMT enzymes vs.
365 eukaryotic ones (including host PMTs), which use distinct lipidic substrates (*i.e.* polyprenol vs. dolichol)
366 (Richards and Hemming, 1972; Babczinski and Tanner, 1973; Verma et al., 1977; Herscovics et al.,
367 1977).

368 More promisingly, our preliminary screening allowed us to identify a small panel of weak MtPMT
369 inhibitors, all containing pyrrole analogs, chosen as biomimetics of short proline-enriched peptides.
370 Indeed, this residue is particularly abundant in the vicinity of mannosylation-sites of mycobacterial
371 glycoproteins (Smith et al., 2014), namely the hydroxyl groups of serine or threonine side chains, as
372 illustrated by the secreted protein rich in Alanine-Proline ("APA"), a major mannosylated antigen of
373 Mtb (Laqueyrie et al., 1995). In particular, our results have led us to consider the two molecules

374 Z66495095 and D-Proline as relevant basic molecular structures for the selection or future design of
375 even more effective inhibitors, with no effect on mycobacterial growth or mannoprotein secretion, in
376 order to avoid the emergence of drug resistance. Remarkably, both of these compounds possess a 5-
377 atom ring, including one nitrogen, and devoid of double bonds. However, it seems that the
378 stereochemistry and the conformation are also important to exert such an inhibitory effect, since
379 remarkably neither L-Proline nor pyrrolidine showed a significant inhibitory effect under the same test
380 conditions. Whether promising or even negative, these results strongly validate the implementation
381 of our MtPMT phenotypic assay for the identification of inhibitors of our mycobacterial target-enzyme.

382 **CONCLUSION AND PERSPECTIVES**

383 Overall, these results provide evidence that our quantitative phenotypic protein-*O*-mannosylation
384 assay is sufficiently robust to detect significant inhibitory effects of MtPMT activity *in mycobacteria*.
385 This assay also appears to be easily adaptable for MtPMT inhibitor screening campaigns at even higher
386 throughput scales, being easily automated and potentially even more miniaturizable. Our preliminary
387 data obtained from the screening of 30 selected compounds supported our hypothesis that the
388 presence of proline near the glycosylation sites of protein substrates probably contributes to their
389 binding to this enzyme, since structurally related compounds inhibit MtPMT activity, probably through
390 a competition effect. This observation therefore encourages us to search in the future, in larger
391 chemical libraries, for potent inhibitors of the molecular recognition between MtPMT and its protein
392 substrates, whose molecular structure could therefore include in priority analogues of pyrrolic rings.
393 Such compounds, capable of preventing the multiplication of *Mtb in-vivo*, by targeting a non-essential
394 virulence factor of mycobacteria with pleiotropic activity, could thus lead to the development of new
395 therapeutic strategies, adjuvant to current anti-tuberculosis treatments, with a reduced risk of
396 inducing bacterial drug-resistance.

397 In the perspective of identifying MtPMT inhibitors capable of crossing the *Mtb* cell wall to reach their
398 membrane-inserted target-enzyme, the results obtained with this MtPMT activity assay in *M.*

399 *smegmatis* could be confirmed directly in pathogenic mycobacteria, by simple transposition of the
400 genetic tools (*i.e.* the plasmids) into Mtb for example. MtPMT inhibitors could then be tested under
401 infection conditions, in cell or mice models. In the future, it might also be interesting to develop similar
402 assays for other relevant biological systems including PMTs. For example, eukaryotes express multiple
403 PMT isoforms that could thus be characterized concomitantly but independently, by co-overexpressing
404 tagged manno-proteins, specific reporter-substrates for each isoform. In particular, this type of assay
405 could be transferred into mammalian reporter cells and applied to the various human PMTs (POMT1/2,
406 TMTC1-4, TMEM260) (Manya et al., 2004; Larsen et al., 2017; Larsen et al., 2023). Differential screening
407 would thus enable assessment of the effects of the mycobacterial hits on host *O*-mannosylation, in
408 order to avoid any undesired inhibition of this vital process. Importantly, the functional data provided
409 by our new phenotypic activity assay allows for a precise analysis of the effects of mutations of MtPMT
410 key amino acids or peptide regions, in an *in-vivo* context. Thus, this assay or its derivatives could also
411 be used to shed light on the modes of molecular interaction between PMT enzymes and their
412 substrates, paving the way for the elucidation of their catalytic mechanism. To achieve this goal, it
413 would also be possible to specifically use the lectin ELLA assay presented in this article to determine
414 more broadly kinetic parameters *in vitro*, and so complete the preliminary work of Cooper et al.
415 (Cooper et al., 2002). Indeed, by using membrane extracts from *M. smegmatis*, this early study showed
416 PMT activities with Km values in the mM range, favored in the presence of Ala residues close to the
417 Thr mannosylation sites of synthetic peptide substrates. Furthermore, the spatial organization and
418 regulation of PMTs could be studied by analyzing their activities resulting from macromolecular
419 complexes similar to those described for oligosaccharyltransferases (Wild et al., 2018), including
420 possible associations as homo- or hetero-oligomers, or with complementary glycosyltransferases,
421 transporters, chaperones, etc., all embedded into their native membrane environment.

422 More generally, GT-C glycosyltransferases are responsible for the production of extracellular glycans
423 involved in many human congenital disorders of glycosylation (Ng and Freeze, 2018), or essential for
424 the virulence of bacterial, viral and protozoan pathogens (Petrou et al., 2016; Puschnik et al., 2017;

425 Yadav and Khan, 2018; Sjodt et al., 2018; Zhang et al., 2020; Ashraf et al., 2022). The development and
426 implementation of miniaturized phenotypic activity assays such as those reported here therefore
427 represent an opportunity to refine our knowledge on the fundamental molecular mechanisms
428 governing GT-C functions, which should stimulate the development of innovative therapeutic
429 strategies targeting these enzymes.

430 **MATERIALS AND METHODS**

431 **Construction of *M. smegmatis* control strains**

432 Construction of the four plasmids pWM19, pMV361, pWM158, and pWM218, was described
433 previously (Malaga et al., 2003; Stover et al., 1991; Liu et al., 2013). The construction of the mutant
434 strain PMM143, was also described previously (Liu et al., 2013). To construct the new PMM186
435 kanamycin-sensitive strain, named Msm- Δ (MsPMT), the res- Ω km-res cassette, was recovered from
436 PMM143 by transforming the latter with the plasmid pWM19 and then selecting a clone with a PCR
437 profile consistent with the res- Ω km-res cassette excision. Plasmids pWM158_L366A, pWM158_Y371A,
438 and pWM158_Y444A were obtained from pWM158, applying Stratagene's QuikChange[®] site-directed
439 mutagenesis method, performed using Phusion DNA polymerase (ThermoFisher) with commercial
440 high-GC buffer, as well as inverted-complementary oligonucleotide-primer pairs containing the desired
441 mutation (**Table I**). All new DNA constructs were validated by restriction profiling and subsequent
442 global sequencing of the entire MtPMT gene, performed by Eurofins Genomics. The strains expressing
443 no PMT, or WT, L366A, Y371A or Y444A MtPMT genes, were constructed by transferring first either
444 the pMV361, or pWM158, pWM158_L366A, or pWM158_Y371A, or pWM158_Y444A plasmids
445 respectively, into the Msm- Δ (MsPMT) strain, and secondly the pWM218 plasmid, as follow.

446 **Transformation and growth conditions of *M. smegmatis* derived strains**

447 *M. smegmatis* cells were grown aerobically overnight at 37°C in Luria-Bertani broth and 0.05% Tween
448 80 (called LBT) until OD_{600nm} = 0.5, followed by 3 washes with cold washing-buffer (0.05% Tween 80,
449 10% glycerol). Electroporation was performed at 2,500 V, 25 μ f, 200 Ω , in the presence of the plasmids
450 pMV361, or pWM158, or pWM158_L366A, or pWM158_Y371A, or pWM158_Y444A, encoding

451 respectively no PMT, or WT, or site-mutated-MtPMT (at ratio 200 ng plasmid/200 μ L cells at OD_{600nm} =
452 25, in washing-buffer). Transformed bacteria were then selected on LB-agar containing 25 μ g/mL
453 kanamycin, and incubated at 37°C for 4 days. Isolated colonies were grown in LBT-kanamycin (25
454 μ g/mL) for 7 days (OD_{600nm} = 0.5), before being transformed with the second plasmid (pWM218,
455 encoding FasC^{His}), plated on LB-agar containing 50 μ g/mL hygromycin, and then grown again for 7-10
456 days in LBT-kanamycin (25 μ g/mL)-hygromycin (50 μ g/mL) (LBT-KH).

457 **LC-ESI-MS analysis of FasC^{His} glycoforms**

458 FasC^{His} was purified from 10-day-old 0.22 μ m-filtered 10 mL flask-culture media of *M. smegmatis*
459 control strains (no PMT, WT, L366A, Y371A, and Y444A), by using Ni-NTA spin columns (Qiagen). The
460 concentration of purified proteins was determined using the Micro BCATM Bicinchoninic Acid Protein
461 Assay Kit (ThermoScientific). SDS-PAGE analyses were performed with 10 μ g protein/well on 13% Tris-
462 glycine-polyacrylamide gels, with a Mini-Protean 3 electrophoresis system (Bio-Rad). Samples were
463 run at 160 V for 1 h. Purified proteins were visualized after staining with InstantBlue (Expedeon),
464 whereas for western-blot analysis, semi-dry transfer onto nitrocellulose membrane was performed (at
465 25 V for 30 min), followed by Anti-Histidine tag detection using a monoclonal-HRP-conjugated antibody
466 (clone 3D5, Invitrogen), following the manufacturer's instructions. NanoLC-MS analyses were
467 performed with 5 μ L of purified proteins diluted in loading buffer (2% acetonitrile (CAN), 0.1% trifluoro
468 acetic acid (TFA)) to final concentration of 0.4 μ M, by employing a nanoRS UHPLC system (Dionex),
469 coupled to a LTQ-Orbitrap Velos mass spectrometer (Thermo Fisher Scientific). Samples were loaded
470 onto a reverse-phase C4 pre-column (300 μ m i.d. x 5mm; Thermo Fisher Scientific) at 20 μ L/min in 2%
471 ACN and 0.05% TFA. After 5 min of desalting, the precolumn was switched online to a home-made C4
472 analytical nanocolumn (75 μ m i.d. x 15 cm) packed with C4 Reprisil (Cluzeau CIL), equilibrated in 95%
473 solvent A (0.2% formic acid (FA)) and 5% solvent B (0.2% FA in ACN). Proteins were eluted using a linear
474 gradient from 5% to 100% B in 38 min, at a flow rate of 300 nL/min. MS scans were acquired in positive
475 mode in the 800-2,000 m/z range with a resolution set at 60,000. The spectra were deconvoluted and
476 semi-quantified with Unidec (10.1021/acs.analchem.5b00140.) using the following parameters: m/z

477 range: 1,000–2,000 Th; no background subtraction, no smoothing; charge range: 10–25; mass range:
478 20,000–30,000 Da; sample mass: every 10 Da; peak detection range: 140 Da, and peak detection
479 threshold: 0.04.

480 **96-well microplate cultures of *M. smegmatis*-derived control strains**

481 After transformation with pWM218, one colony of each *M. smegmatis* control strain was transferred
482 into 10 mL LBT-KH medium in a flask. After 4 days, 10 mL of fresh LBT-KH were added, and culture
483 prolonged for 3 additional days until OD_{600nm} 1.5. In order to inoculate the wells with a homogeneous
484 aggregate-free bacterial suspension, the 20 mL pre-culture was centrifuged for 10 min at 4°C, at 500
485 g. 5 sterile glass beads (4 mm) were added to the pellet to gently dislodge it. 20 mL of cold Luria-Bertani
486 Tween medium (LBT) were added, then the clear suspension was centrifuged for 10 min at 100 g,
487 harvested and assayed at OD_{600nm}. Duplicate microplates were then inoculated at OD_{600nm} 0.1 in 250
488 µL/well of LBT-Kanamycin-Hygromycin (LBT-KH). Plastic covers were placed on the microplates to limit
489 medium evaporation. Microplates were incubated at 37°C in a humidity-controlled oven. OD_{600nm} was
490 measured with the BMG LABTECH Clariostar, after homogenizing 25 µL/well of culture in 75 µL of mQ
491 water, by gentle pipetting/filling. Further direct- and/or lectin-ELISA analyses could then be performed
492 from culture supernatants, obtained by centrifugation of the whole microplates at 2,000 g at 4°C for
493 15 min.

494 **Direct quantification of FasC^{His} concentration and mannosylation from microculture supernatants**

495 For both assays, supernatants were analyzed in triplicate in 96-well microplates. FasC^{His} concentrations
496 were determined by Direct Anti-His tag ELISA. A standard range from 50 to 2,000 ng/mL (in PBS) of
497 purified FasC^{His} was prepared for each microplate. 50 µL/well of culture supernatant, diluted 100x in
498 PBS, were mixed with 50 µL/well of carbonate coating-buffer (Na₂CO₃ 0.53%/NaHCO₃ 0.42%, pH 9.6)
499 and then incubated overnight at room temperature. After washing 3 times with 200 µL/well PBS, the
500 plates were incubated for 1 h at room temperature with 200 µL/well PBS containing 0.05% Tween 20
501 and 5% milk. After 3 washes with 200 µL/well of PBS containing 0.05% Tween 20, the plate was

502 incubated for 2 h at room temperature with 50 μ L/well of anti-His antibody (anti-His C-term-HRP
503 antibody, Invitrogen), diluted 1,000x in PBS containing 0.05% Tween 20 and 0.5% milk. Four washes
504 with 200 μ L/well of PBS were performed before revelation.

505 Quantifications of FasC^{His} mannosylation were determined by enzyme linked lectin assay (ELLA). For
506 this assay, 96-well microplates coated with anti-His antibody (Genscript) were used. 100 μ L/well of
507 culture-supernatants (diluted twice in PBS) were placed in the wells. The plate was incubated for 3 h
508 at room temperature and then washed 4 times with 260 μ L/well of PBS containing 2% Tween 20. 100
509 μ L of Concanavalin A-HRP solution (0.5 μ g/mL ConA-HRP, 1 mM CaCl₂, 1 mM MgCl₂, 1 mM MnCl₂,
510 0.05% Tween20, in PBS) were added and then the plate was incubated at room temperature for 2 h
511 and washed 4 times with 260 μ L/well of PBS. Values of 100% and 0% were defined as the ones
512 measured for the WT and No PMT *M. smegmatis* control strains, respectively.

513 For both assays, revelation was performed with 50 μ L/well of TMB solution (eBioscience). 25 μ L/well
514 of stop solution (1 mM sulfuric acid) was added after 20 min incubation. Absorbances were measured
515 at 450 nm using the BMG LABTECH Clariostar microplate reader. Saturation of the pre-coated anti-
516 histidine antibody of the ELLA was ensured from at least 200 ng/well of FasC^{His}, amount possibly
517 inferred from concentrations determined by Direct-ELISA.

518 **Cell treatment with putative MtPMT inhibitors**

519 Microplates were inoculated at OD_{600nm} 0.1 in 250 μ L/well of LBT-KH, in the presence of 2.5 μ L of 100x-
520 concentrated compound (prepared in DMSO, then added into wells at final concentrations ranging
521 from 2.5 to 250 μ M) and then incubated at 37°C for 7 days in a humidity-controlled oven. The
522 microcultures in rows A and H, as well as columns 1, 2, and 12 were not treated with any compound,
523 nor were they analyzed, to avoid considering possible "edge effects." The wells in row D and column 7
524 were filled with compound-free DMSO to allow data normalization by the values obtained for these
525 "untreated" microcultures. The microcultures in row E were inoculated with the No PMT strain to serve
526 as blank for the ELLA assay.

527 **Statistical analysis of the effects of MtPMT inhibitors**

528 The statistical analysis of the effect of varying concentrations of D-Proline, Z317129322, or Z66495095
529 on ConA binding was carried out in R, v4.2.1 (RCoreTeam, 2022), using the default *stats* package to
530 perform a full two-way ANCOVA where the concentration of the molecule was used as numeric
531 covariable. Data handling and graphic output of the result was produced using *dplyr*, *tidyr*,
532 and *ggplot2* packages, all within the *tidyverse* metapackage, v2.0.0 (Wickham et al., 2019). R codes are
533 available upon request.

534 **Screened compounds**

535 - Pyrrole derivatives: the following compounds were obtained from the commercial suppliers
536 indicated below and used without further purification.

- 537 ○ 7 compounds from Sigma-Aldrich : D-Proline (Ref. 858919, CAS 344-25-2, synonyme
538 (R)-Pyrrolidine-2-carboxylic acid), L-Proline (Ref. P0380, CAS 147-85-3, synonyme (S)-
539 Pyrrolidine-2-carboxylic acid), S-2-Pyrrolidinemethanol (Ref. 186511, CAS 23356-96-9,
540 synonyme (S)-(+)-2-(Hydroxymethyl)pyrrolidine), Pyrrolidine (Ref. 83240, CAS 123-75-
541 1, synonyme Tetrahydropyrrole), Linezolid (Ref. PZ0014, CAS 165800-03-3, synonyme
542 N-[[[(5S)-3-[3-Fluoro-4-(4-morpholinyl)phenyl]-2-oxo-5
543 oxazolidinyl]methyl]acetamide), Ac-TGP-trifluoroacetate (Ref. A2112, CAS 292171-04-
544 1, synonyme 1-Acetyl-L-prolylglycyl-L-proline), KYP-247 (Ref. SML0208, CAS 796874-
545 99-2, synonyme (2S)-1-[[[(2S)-1-(1-Oxo-4-phenylbutyl)-2-pyrrolidinyl]carbonyl]-2-
546 pyrrolidinecarbonitrile)
- 547 ○ 7 compounds from Enamine, provided by the PICT platform (IPBS, Toulouse) :
548 Z327500930 (CAS 1208771-15-6, IUPAC 2-[[5-amino-4-(prop-2-en-1-yl)-4H-1,2,4-
549 triazol-3-yl]sulfanyl]-N-(prop-2-yn-1-yl)acetamide); Z21489961 (CAS 920849-58-7,
550 IUPAC 1-[2,5-dimethyl-1-(1,3-thiazol-2-yl)-1H-pyrrol-3-yl]-2-[[5-(pyridin-4-yl)-1,3,4-
551 oxadiazol-2-yl]sulfanyl]ethan-1-one); Z280700946 (CAS 1007750-34-6, IUPAC 2-(3-
552 cyano-1H-1,2,4-triazol-1-yl)-N-(cyclopent-1-en-1-yl)-N-methylacetamide); Z56816758

553 (CAS 380311-07-9, IUPAC 2-[(4-methylpyrimidin-2-yl)sulfanyl]-1-(thiophen-2-
554 yl)ethan-1-one); Z269692472, no CAS, IUPAC 3-[(1E)-2-(5-methylfuran-2-yl)ethenyl]-
555 5-[(2-methylprop-2-en-1-yl)sulfanyl]-4H-1,2,4-triazole); Z317129322 (no CAS, IUPAC
556 5-(2-methylpropyl)-3-[[3-[(1E)-2-(thiophen-2-yl)ethenyl]-1H-1,2,4-triazol-5-
557 yl}sulfanyl)methyl]-1,2,4-oxadiazole); Z66495095 (no CAS, IUPAC (2E)-3-[2,5-dimethyl-
558 1-(5-methyl-1,2-oxazol-3-yl)-1H-pyrrol-3-yl]-1-[2-(thiophen-2-yl)pyrrolidin-1-yl]prop-
559 2-en-1-one)

560 - Rhodamine derivatives: the following compounds were obtained from collaborators indicated
561 below and used without further purification. The 2 yeast inhibitors called OGT2599 or R3A-5a
562 were kindly supplied respectively by Dr. Joachim F. Ernst, Heinrich-Heine-Universität
563 Düsseldorf and Dr. Sabine Strahl, Ruprecht-Karls-University Heidelberg while the 2 compounds
564 with bactericidal activity on latent Mtb called D155931 and D157070 (Bryk et al., 2008) were
565 kindly provided by Dr. Carl F. Nathan, (Cornell University, USA).

566 - The remaining rhodamine-containing compounds (474705Z01, 477335Z01, 474841Z01,
567 474737Z01, 466243Z01, 463271Z01, 478185Z01) were obtained from collaborators and were
568 blind tested.

569 - Glycosyltransferase inhibitors of the transition state mimic class: TK220, TK203, TK292, JSPB,
570 S70-2 were proposed by collaborators for blind testing.

571 **FUNDING**

572 This work was supported by the Fondation pour la Recherche Médicale (Equipes FRM
573 DEQ20180339208 to Nigou J.), the Fondation MSDAVENIR (grant FIGHT-TB to Nigou J.), the Fondation
574 Rolland Garrigou pour la culture et la santé (FONROGA, supporting this work for Master internship
575 grant), and the Agence Nationale de la Recherche (grant ANR-20-PAMR-0005 to Nigou J.). This work
576 was also funded in part by grants from the Région Occitanie, European funds (FEDER, Fonds Européens
577 de Développement Régional), Toulouse Métropole, and the French ministry of research with the

578 Investissement d'Avenir Infrastructures Nationales en Biologie et Santé program (ProFI, Proteomics
579 French Infrastructure project, ANR-10-INBS-08).

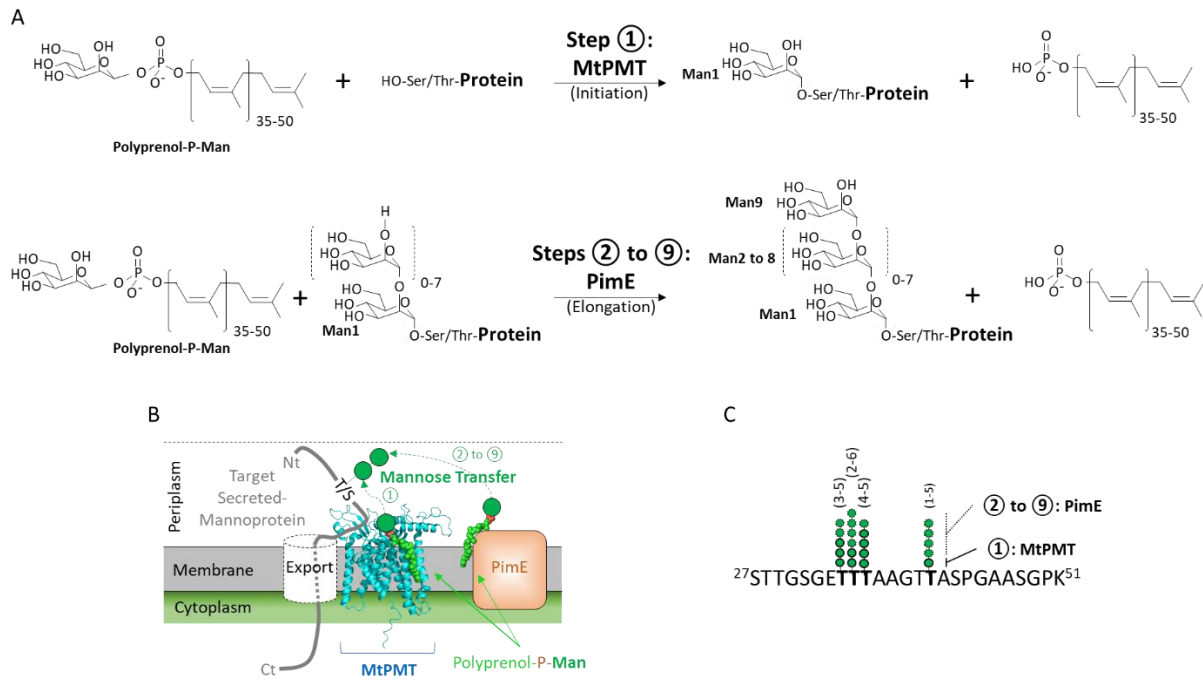
580 **ACKNOWLEDGMENTS**

581 We thank the staff from the Institute of Pharmacology and Structural Biology, for their help throughout
582 this work; Wladimir Malaga and Dr Christian Chalut (team "Molecular Mycobacterial Pathogenesis",
583 directed by Dr Christophe Guilhot) for providing the original plasmids (pWM158, pMV361, pWM218)
584 and strains (PMM143 and PMM186), and their precious advice for the engineering of the
585 mycobacterial strains; Pascal Ramos for technical assistance in the preparation and validation of the
586 chemical compounds provided by the Integrated Screening Platform of Toulouse (PICT, IBISA); staff
587 from the Genotoul Biostat Platform.

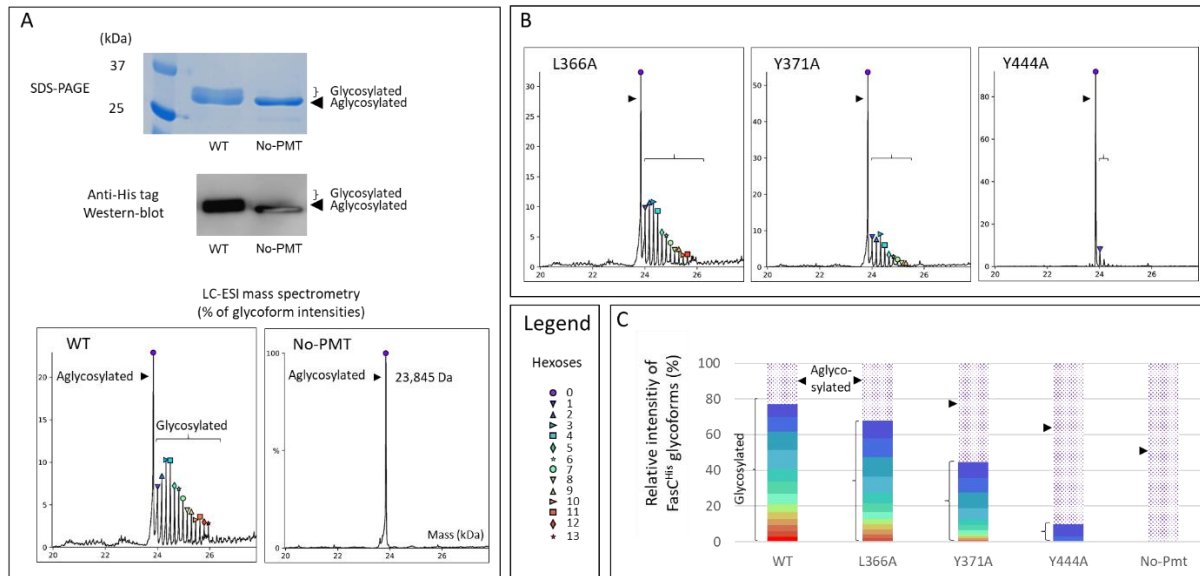
588 **ABBREVIATIONS**

| | | |
|-----|---------------------|--|
| 589 | APA | Alanine-Proline rich antigen, Rv1860 |
| 590 | ConA-HRP | Concanavalin A conjugated to horseradish peroxidase |
| 591 | ELLA | Enzyme linked lectin assay |
| 592 | ELISA | Enzyme linked immunosorbent assay |
| 593 | FasC ^{His} | Fasciclin, encoded by the MSMEG_5196 gene, fused C-terminally with a 594 <i>6xhistidine</i> tag |
| 595 | Polyprenol-P-Man | Polyprenol-Phosphate-activated mannose |
| 596 | LBT-KH | Luria-Bertani-Tween broth complemented with kanamycin and hygromycin |
| 597 | LC | Liquid Chromatography |
| 598 | MS | Mass Spectrometry |
| 599 | Mtb | <i>Mycobacterium tuberculosis</i> |
| 600 | MtPMT | Protein-O-Mannosyltransferase from <i>Mycobacterium tuberculosis</i> |
| 601 | SDS-PAGE | Sodium Dodecyl Sulfate PolyAcrylamide Gel Electrophoresis |
| 602 | SEM | Standard Error of the Mean |

| | | |
|-----|-----|--------------------------------|
| 603 | TMB | 3,3',5,5'-tetramethylbenzidine |
| 604 | WT | Wild-type |
| 605 | | |



608 **Figure 1. MtPMT and PimE enzymatic activities in *Mycobacterium tuberculosis* (Mtb).** A- Reactions
 609 successively catalyzed by the two enzymes. B- Representation of the protein-*O*-mannosylation
 610 process. C- Example of repertoire of proteoglycoforms of peptide P₂₇₋₅₁ from LpqH (Parra et al., 2017).
 611 The Protein-*O*-mannosyltransferase MtPMT catalyzes the transfer of initial mannose units from
 612 polyprenol-phosphate-activated mannose (Polyprenol-P-Man) to the hydroxyls of Threonine or Serine
 613 residues (T/S) of secreted or membrane mycobacterial mannoproteins (VanderVen et al., 2005; Tonini
 614 et al., 2020). Then, the mannosyltransferase PimE would be responsible for the stepwise elongation of
 615 oligomannosyl appendages (Liu et al., 2013). These two processes are probably co-translational, as
 616 suggested by analogies with eukaryote protein-*O*-mannosylation machinery (VanderVen et al., 2005;
 617 Loibl et al., 2014).



630

631

632

633

634

635

636 **Figure 3. Comparison of different purified FasC^{His} proteins with disrupted glycosylation patterns.**

637 FasC^{His} proteins were purified from 10-day flask culture supernatants of distinct *M. smegmatis*

638 Δ (MsPMT) strains expressing the wild-type (WT), or mutated (L366A, Y371A, Y444A), or no PMT genes.

639 The FasC^{His} from the different strains were compared in terms of glycosylation profiles observed either

640 after electrophoresis, or from deconvoluted spectra obtained by denaturing nano-LC-ESI-MS. A-

641 Electrophoretic and deconvoluted spectra obtained for the WT and No-PMT strains. B- Deconvoluted

642 spectra obtained for the L366A, Y371A and Y444A strains. C- Overall quantitative comparison of the

643 glycosylation patterns, inferred from the LC-ESI-MS analysis (shown in A and B). The legend indicates

644 for each peak the number of hexoses linked to the protein, deduced from the corresponding molecular

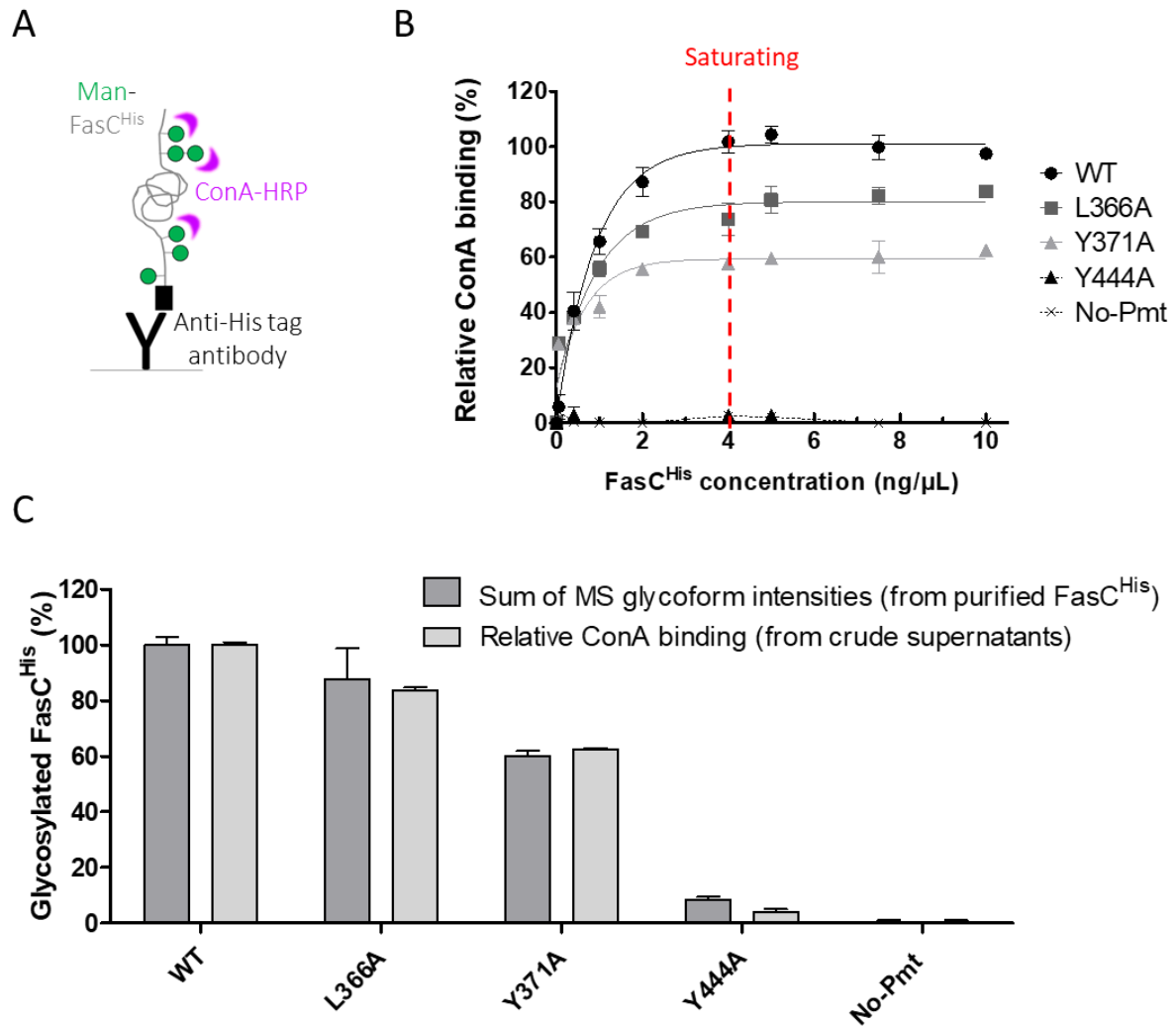
645 weight. Relative intensities are represented for each of these glycoforms, normalized with the sum of

646 intensities of all the observed species. In each panel, the aglycosylated form of FasC^{His}, present in all

647 strain supernatants, is designated by an arrow. The different glycosylated forms of FasC^{His} are indicated

648 by a bracket.

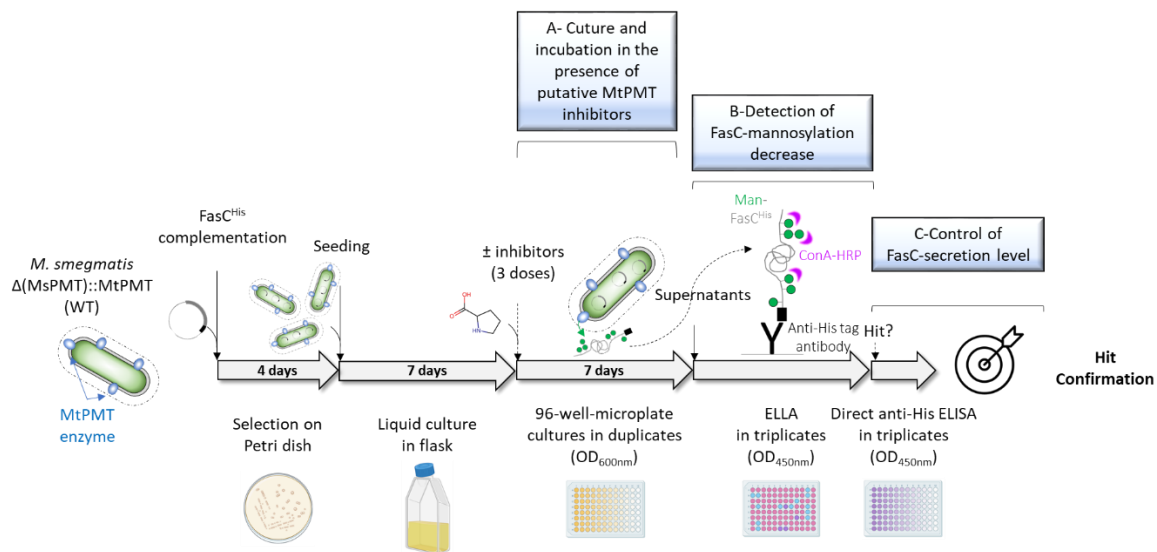
649



650
651
652
653
654
655
656
657
658
659
660
661
662
663
664
665
666

Figure 4. Validation of the enzyme linked lectin assay (ELLA), for the quantification of FasC^{His} glycosylation from microplate-culture crude supernatants. Reporter substrates produced from different strains of *M. smegmatis* Δ (MsPMT) expressing either the WT-MtPMT, or mutated (L366A, Y371A, Y444A) MtPMT, or no (No-PMT) genes, were compared. A-Principle of the ELLA. This test involved 96-well microplates, pre-coated with anti-His tag antibodies, to allow the capture of tagged FasC^{His} from supernatants. Binding with Concanavalin A conjugated to horseradish peroxidase (ConA-HRP), able to link terminal mannose residues (symbolized as green spheres), was quantified using the 3,3',5,5'-tetramethylbenzidine (TMB) ELISA-substrate. B- ELLA analysis for increasing loading-rates of FasC^{His}. The ConA binding values (%) were determined as the intensities of ConA-HRP signals, obtained for gradually diluted supernatants. C- Correlation between quantitative results obtained by LC-ESI-MS analysis (with intensities of all glycoforms summed and normalized to WT), and ConA binding values determined by ELLA (for saturating loading amounts of FasC^{His}). Values of 100% and 0% were defined as the ones measured for strains expressing the WT-MtPMT or No-PMT genes, respectively. Biological duplicates, analyzed in technical triplicates, are presented.

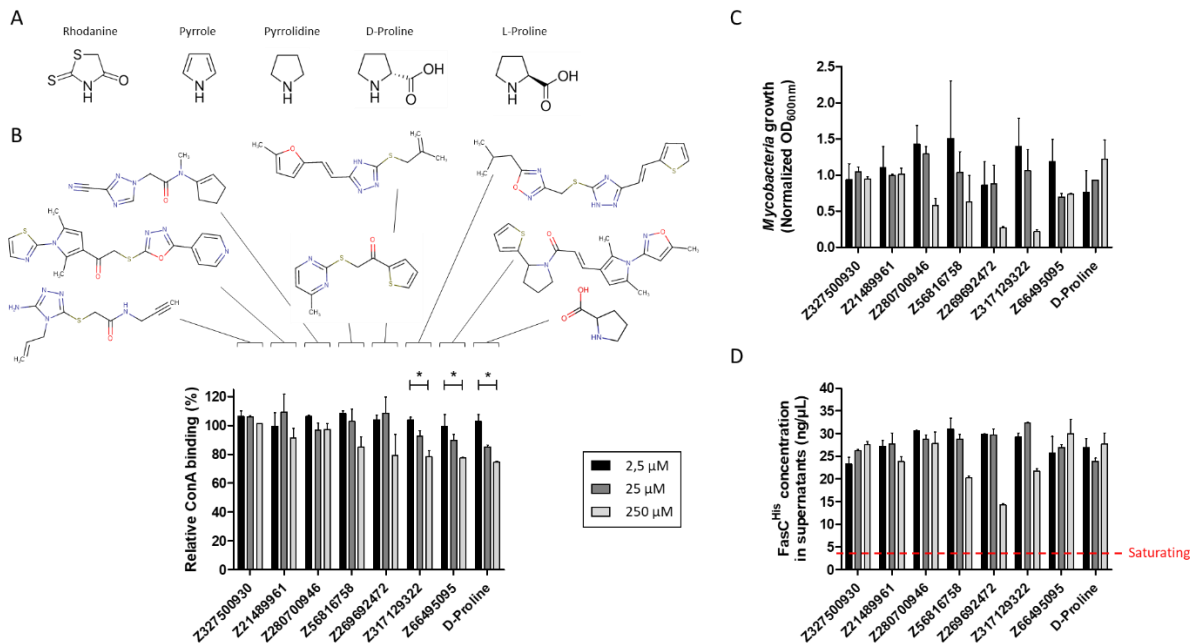
667
668
669



670
671
672
673
674
675
676
677
678
679
680
681
682
683
684
685
686
687
688
689

Figure 5. Workflow of the MtPMT phenotypic assay. A- The *M. smegmatis* $\Delta(\text{MsPMT})$ strain permanently expressing the WT-MtPMT gene, was complemented with the plasmid coding for high-level transient expression of FasC^{His} . After selection on a Petri dish in the presence of appropriate antibiotics, one colony of this fresh activity reporter-strain was transferred into liquid medium. After 7 days of culture in a flask, microplates were then inoculated in the presence of the putative MtPMT inhibitors at varying concentrations. B- After 7 days of culture, the OD_{600nm} was measured and the supernatants were collected in order to quantify FasC^{His} mannosylation, by ELLA. This assay inherently allowed for normalization of the FasC^{His} concentrations between wells, necessary to compare FasC mannosylation levels, thanks to the saturation of the pre-coated anti-His tag antibody. C- Whenever a decrease in FasC mannosylation was detected, the identification of the corresponding chemical compound as a "hit" was conditioned to an additional control of FasC^{His} concentration in culture supernatants, by direct-anti-His tag ELISA, to ensure that the conditions of anti-His antibody saturation had been reached in the previous ELLA test.

690
691
692

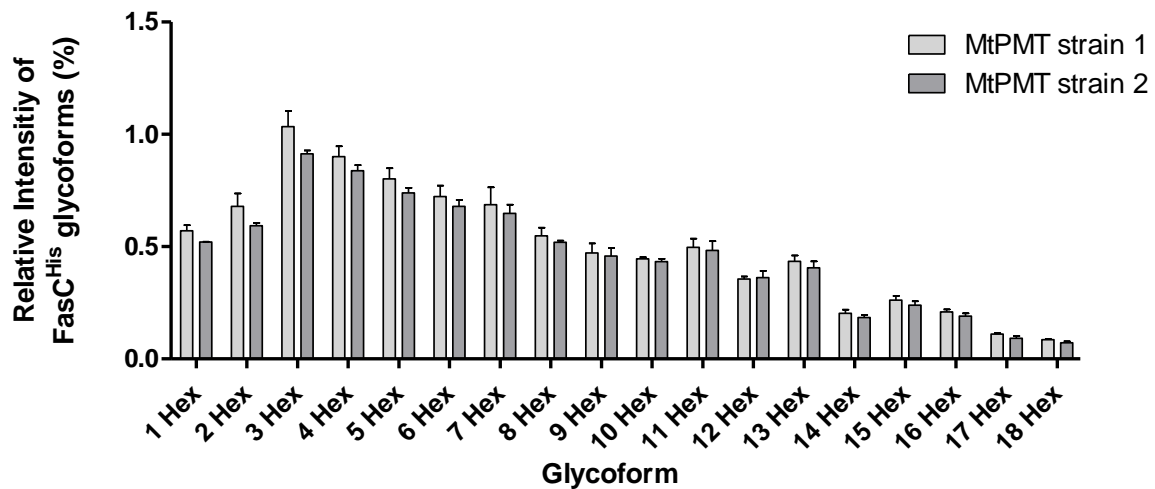


693
694
695

696 **Figure 6. Implementation of the MtPMT phenotypic assay.** Dose-response effects of different pyrrolic
697 derivatives were observed from extracts of 7-day 96-well microcultures of the "WT-MtPMT activity
698 reporter-strain", after treatment with the indicated concentrations of compounds (see box). A-
699 Structure of the different cyclic compounds mentioned in this study. B- Effects on FasC^{His}
700 mannosylation, deduced from ELLA analysis. Supernatant ConA-HRP binding signals (%), normalized to
701 the signal obtained for representative wells of the untreated strain, in the presence of saturating
702 loading-amounts of FasC^{His}. C- Effects on bacterial growth. OD_{600nm} of culture samples, normalized to
703 the average obtained for four representative wells of the untreated strain. D- Effects on FasC^{His}
704 secretion, deduced from direct anti-His ELISA analysis. Data are presented as the mean ± standard
705 error of the mean (SEM) of two independent biological replicates (or a single representative
706 experiment in D), of which 3 technical replicates were performed. Stars summarize the results of the
707 ANCOVA analysis (n=2), highlighting statistically significant differences in terms of *p*-values (*: *p*-
708 value ≤ 0.00002), between compound concentrations from 2.5 μM to 250 μM (see **Sup. fig. 4**).

709
710
711
712

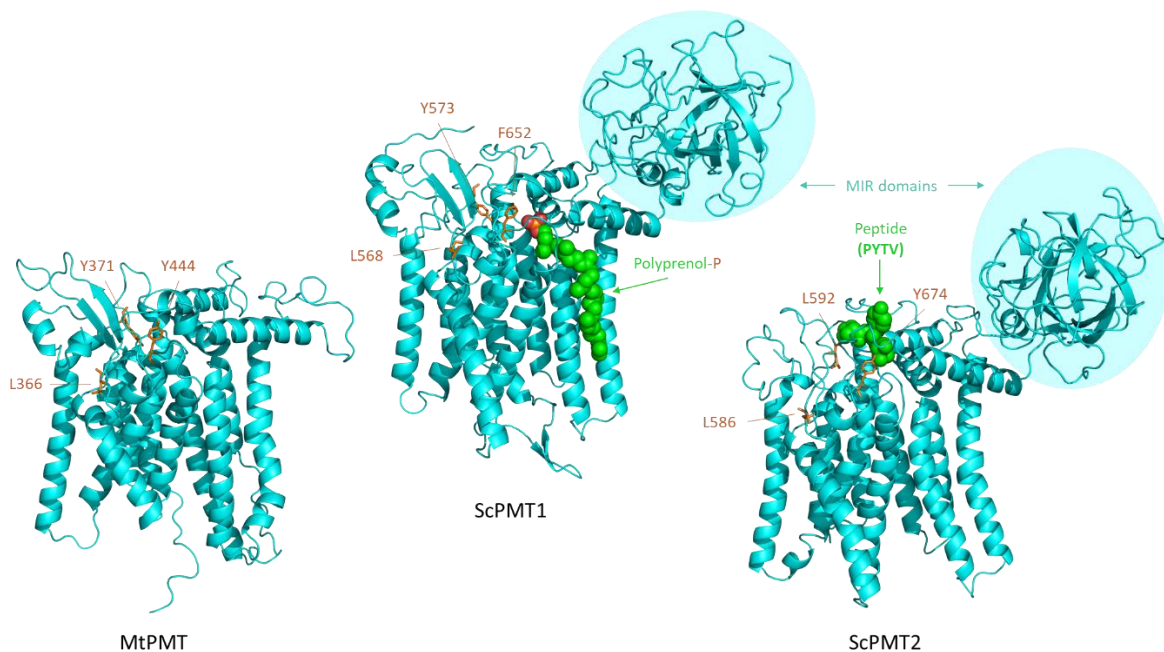
Supplementary Figures



714

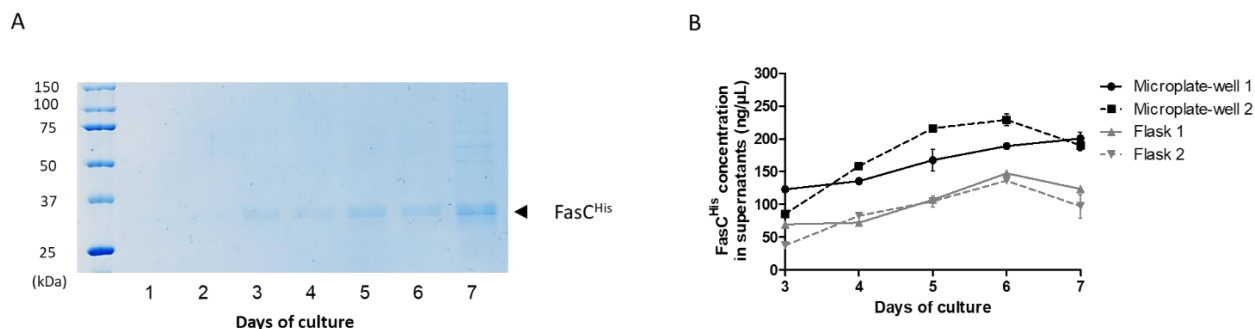
715 Supplementary figure 1. Reproducibility validation of LC-ESI-MS analysis of FasC^{His} glycoforms. The
 716 reporter-substrate mannoprotein was purified from supernatants of 10-day-old flask cultures of the
 717 WT-MtPMT activity reporter strain. Relative intensities of glycoform peaks (normalized to the intensity
 718 of the aglycosylated form, 0 Hex) are shown for two biological duplicates, analyzed as technical
 719 duplicates.

720



721

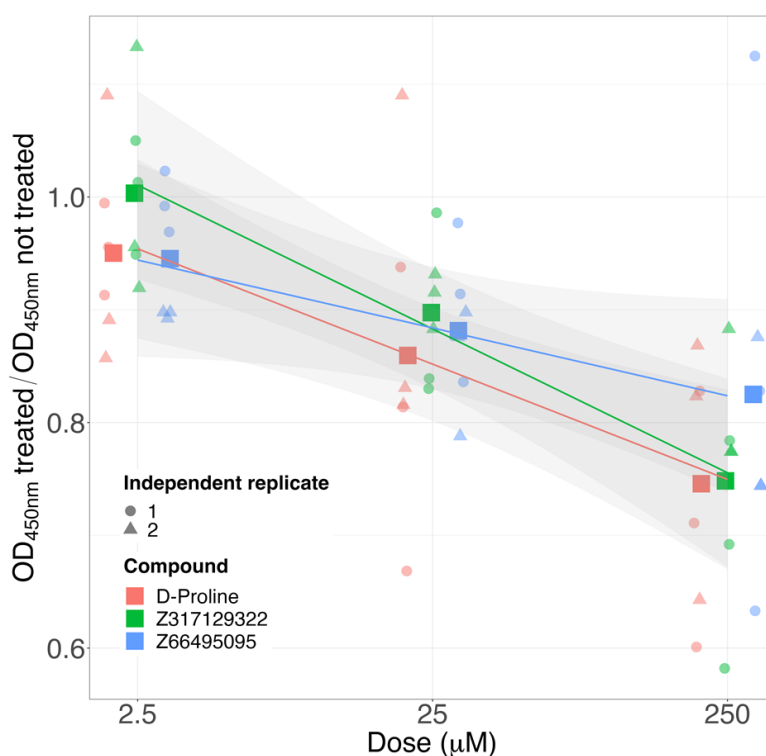
722 Supplementary figure 2. Homologous structures of MtPMT, ScPMT1 and ScPMT2. The AlphaFold model
 723 of MtPMT as well as the cryo-EM structures of ScPMT1 and 2, in complex with donor and acceptor
 724 substrates respectively (Bai et al., 2019) are shown (cyan cartoons, with the substrates as red and
 725 green spheres). Mutated amino acid residues in MtPMT during this study, as well as aligning amino
 726 acids in ScPMT1/2 sequences, are represented as orange sticks. MIR domains are absent in MtPMT but
 727 present in eukaryote PMTs such as ScPMT1/2.



728

729 Supplementary figure 3. Monitoring of FasCHis enrichment in crude supernatants from 96-well
 730 microplate cultures. The MtPMT activity reporter strain was cultured over seven days. A- SDS-PAGE
 731 analysis. 10 μ L of supernatant, collected each day of culture, were loaded per lane. B- Direct anti-
 732 6xHis tag ELISA analysis; comparison with cultures in flasks. Biological duplicates, analyzed in
 733 technical triplicates, are presented.

734



735

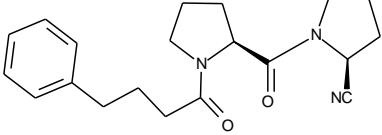
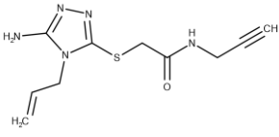
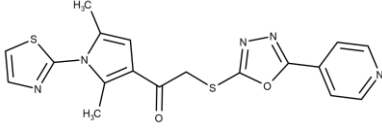
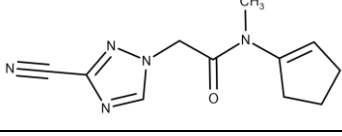
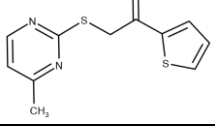
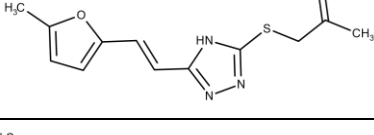
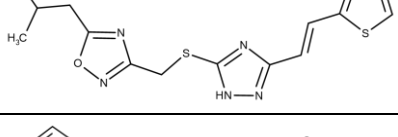
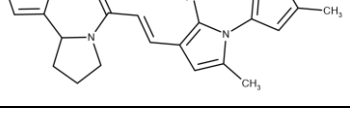
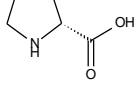
736 Supplementary figure 4. Significance of MtPMT-activity in-bacteria inhibitions, detected by applying
 737 the ELLA assay. The dose-response effect of the 3 compounds Z317129322, Z66495095, and D-
 738 Proline, were observed after treatment of cells with the indicated concentrations. Normalized ConA-
 739 HRP binding signals (OD450nm), obtained from microculture supernatants containing saturating
 740 concentrations of FasCHis, are presented. Data from two-independent biological replicates are
 741 shown (circles vs. triangles), of which 3 technical triplicates were performed. Squares represent the
 742 mean values from the two independent experiments. Red, D-Proline ; green, Z317129322 ; blue,
 743 Z66495095. Straight-lines represent dose-wise linear regressions of normalized OD450nm for each of
 744 the three compounds, and grey areas represent the SEM of each of those regressions. The two-way
 745 ANCOVA analysis revealed that the effect of the dose was significant (p -value = $1.04 \cdot 10^{-5}$, $n = 2$),
 746 with no significant differences between the three compounds.

747 **Table I.** Name and main features of sense-primers, plasmids and strains used in this study

| Name | Relevant characteristics | Trivial name | Antibiotic resistance | Source |
|---|---|---------------------------------------|---------------------------|-----------------------|
| Sequences of sense-primers (5'-3') | | | | |
| Sp-L366A | CC TGG CCC ATG GCG TTG CGG CCG GTG CTC TAC GCC ATC G | | | This study |
| Sp-Y371A | G TTG CGG CCG GTG CTC GCC GCC ATC GAC CAG | | | This study |
| Sp-Y444A | GCC GAC ATC GAT CGG CAG ATG GCC TTC TTC TAC | | | This study |
| Plasmids | | | | |
| pWM19 | Thermosensitive <i>Escherichia coli</i> /mycobacteria shuttle plasmid containing the resolvase gene from transposon $\gamma\delta$ | Res | Hygromycin and Gentamicin | (Malaga et al., 2003) |
| pMV361 | Integrative <i>Escherichia coli</i> /mycobacteria shuttle vector | Empty | Kanamycin | (Stover et al., 1991) |
| pWM158 | Mycobacterial integrative plasmid, derived from pMV361, containing the wild-type MtPMT gene from <i>Mtb</i> (Rv1002c) under the control of the pBlaF* promoter | WT-MtPMT | Kanamycin | (Liu et al., 2013) |
| pWM158_L366A | derived from pWM158, containing the L366A-mutated-MtPMT gene from <i>Mtb</i> | L366A-MtPMT | Kanamycin | This study |
| pWM158_Y371A | derived from pWM158, containing the Y371A-mutated-MtPMT gene from <i>Mtb</i> | Y371A-MtPMT | Kanamycin | This study |
| pWM158_Y444A | derived from pWM158, containing the Y444A-mutated-MtPMT gene from <i>Mtb</i> | Y444A-MtPMT | Kanamycin | This study |
| pWM218 | Mycobacterial replicative plasmid containing the FasC^{His} gene under the control of the pBlaF* promoter | FasCHis | Hygromycin | (Liu et al., 2013) |
| Strains | | | | |
| PMM143 | <i>M. smegmatis</i> mc ² 155 Msmeg_5447::res- Qkm-res | Msm- Δ (MsPMT)_km ^R | Kanamycin | (Liu et al., 2013) |
| PMM186 | <i>M. smegmatis</i> mc ² 155 Msmeg_5447::res | Msm- Δ (MsPMT) | - | This study |
| PMM186::pMV361:pWM218 | PMM186 transformed with pMV361 and pWM218 | No PMT | Kanamycin and Hygromycin | This study |
| PMM186::pWM158:pWM218 | PMM186 transformed with pWM158 and pWM218 | WT | Kanamycin and Hygromycin | This study |
| PMM186::pWM158_L366A:pWM218 | PMM186 transformed with pWM158_L366A and pWM218 | L366A | Kanamycin and Hygromycin | This study |
| PMM186::pWM158_Y371A:pWM218 | PMM186 transformed with pWM158_Y371A and pWM218 | Y371A | Kanamycin and Hygromycin | This study |
| PMM186::pWM158_Y444A:pWM218 | PMM186 transformed with pWM158_Y444A and pWM218 | Y444A | Kanamycin and Hygromycin | This study |

748

749

| | | | |
|---|------------|--|---|
| | KYP-247 |  | |
| Glycosyl-transferase inhibitors | TK220 | Unrevealed | Collaborators (blind-tested) |
| | TK203 | Unrevealed | |
| | TK292 | Unrevealed | |
| | JSPB | Unrevealed | |
| | S70-2 | Unrevealed | |
| 8 compounds with inhibitory effect on MtPMT activity | | | |
| Pyrrrole derivatives | Z327500930 |  | Enamine |
| | Z21489961 |  | |
| | Z280700946 |  | |
| | Z56816758 |  | |
| | Z269692472 |  | |
| | Z317129322 |  | |
| | Z66495095 |  | |
| | | D-Proline |  |

751

752

753 **REFERENCES**

- 754 Alonso, H., Parra, J., Malaga, W., Payros, D., Liu, C. F., Berrone, C., Robert, C., Meunier, E., Burlet-Schiltz,
755 O., Riviere, M., and Guilhot, C. (2017). Protein O-mannosylation deficiency increases LprG-associated
756 lipoarabinomannan release by *Mycobacterium tuberculosis* and enhances the TLR2-associated
757 inflammatory response. *Sci Rep* 7, 7913.
- 758 Argyros, R., Nelson, S., Kull, A., Chen, M. T., Stadheim, T. A., and Jiang, B. (2013). A phenylalanine to
759 serine substitution within an O-protein mannosyltransferase led to strong resistance to PMT-inhibitors
760 in *Pichia pastoris*. *PLoS One* 8, e62229.
- 761 Arroyo, J., Hutzler, J., Bermejo, C., Ragni, E., Garcia-Cantalejo, J., Botias, P., Piberger, H., Schott, A.,
762 Sanz, A. B., and Strahl, S. (2011). Functional and genomic analyses of blocked protein O-mannosylation
763 in baker's yeast. *Mol Microbiol* 79, 1529-1546.
- 764 Ashraf, K. U., Nygaard, R., Vickery, O. N., Erramilli, S. K., Herrera, C. M., McConville, T. H., Petrou, V. I.,
765 Giacometti, S. I., Dufresne, M. B., Nosol, K., Zinkle, A. P., Graham, C. L. B., Loukeris, M., Kloss, B.,
766 Skorupinska-Tudek, K., Swiezewska, E., Roper, D. I., Clarke, O. B., Uhlemann, A. C., Kosiakoff, A. A.,
767 Trent, M. S., Stansfeld, P. J., and Mancía, F. (2022). Structural basis of lipopolysaccharide maturation
768 by the O-antigen ligase. *Nature* 604, 371-376.
- 769
- 770 Babczinski, P., and Tanner, W. (1973). Involvement of dolicholmonophosphate in the formation of
771 specific mannosyl-linkages in yeast glycoproteins. *Biochem Biophys Res Commun* 54, 1119-1124.
- 772
- 773 Bai, L., Kovach, A., You, Q., Kenny, A., and Li, H. (2019). Structure of the eukaryotic protein O-
774 mannosyltransferase Pmt1-Pmt2 complex. *Nat Struct Mol Biol* 26, 704-711.
- 775 Bryk, R., Gold, B., Venugopal, A., Singh, J., Samy, R., Pupek, K., Cao, H., Popescu, C., Gurney, M., Hotha,
776 S., Cherian, J., Rhee, K., Ly, L., Converse, P. J., Ehrhart, S., Vandal, O., Jiang, X., Schneider, J., Lin, G., and
777 Nathan, C. (2008). Selective killing of nonreplicating mycobacteria. *Cell Host Microbe* 3, 137-145.
- 778 Cantero, P. D., Lengsfeld, C., Prill, S. K., Subanovic, M., Roman, E., Pla, J., and Ernst, J. F. (2007).
779 Transcriptional and physiological adaptation to defective protein-O-mannosylation in *Candida*
780 *albicans*. *Mol Microbiol* 64, 1115-1128.
- 781 Carr, M. D., Bloemink, M. J., Dentten, E., Whelan, A. O., Gordon, S. V., Kelly, G., Frenkiel, T. A.,
782 Hewinson, R. G., and Williamson, R. A. (2003). Solution structure of the *Mycobacterium tuberculosis*
783 complex protein MPB70: from tuberculosis pathogenesis to inherited human corneal disease. *J Biol*
784 *Chem* 278, 43736-43743.
- 785 Chao, L., and Jongkees, S. (2019). High-Throughput Approaches in Carbohydrate-Active Enzymology:
786 Glycosidase and Glycosyl Transferase Inhibitors, Evolution, and Discovery. *Angew Chem Int Ed Engl* 58,
787 12750-12760.
- 788 Clatworthy, A. E., Pierson, E., and Hung, D. T. (2007). Targeting virulence: a new paradigm for
789 antimicrobial therapy. *Nat Chem Biol* 3, 541-548.
- 790 Cooper, H. N., Gurucha, S. S., Nigou, J., Brennan, P. J., Belisle, J. T., Besra, G. S., and Young, D. (2002).
791 Characterization of mycobacterial protein glycosyltransferase activity using synthetic peptide
792 acceptors in a cell-free assay. *Glycobiology* 12, 427-434.
- 793 Dobos, K. M., Swiderek, K., Khoo, K. H., Brennan, P. J., and Belisle, J. T. (1995). Evidence for glycosylation
794 sites on the 45-kilodalton glycoprotein of *Mycobacterium tuberculosis*. *Infect Immun* 63, 2846-2853.

795 Esparza, M., Palomares, B., Garcia, T., Espinosa, P., Zenteno, E., and Mancilla, R. (2015). PstS-1, the 38-
796 kDa *Mycobacterium tuberculosis* glycoprotein, is an adhesin, which binds the macrophage mannose
797 receptor and promotes phagocytosis. *Scand J Immunol* 81, 46-55.

798 Garbe, T., Harris, D., Vordermeier, M., Lathigra, R., Ivanyi, J., and Young, D. (1993). Expression of the
799 *Mycobacterium tuberculosis* 19-kilodalton antigen in *Mycobacterium smegmatis*: immunological
800 analysis and evidence of glycosylation. *Infect Immun* 61, 260-267.

801 Gigante, V., Sati, H., and Beyer, P. (2022). Recent advances and challenges in antibacterial drug
802 development. *Admet Dmpk* 10, 147-151.

803 Girrbach, V., Zeller, T., Priesmeier, M., and Strahl-Bolsinger, S. (2000). Structure-function analysis of
804 the dolichyl phosphate-mannose: protein O-mannosyltransferase ScPmt1p. *J Biol Chem* 275, 19288-
805 19296.

806 Herscovics, A., Golovtchenko, A. M., Warren, C. D., Bugge, B., and Jeanloz, R. W. (1977).
807 Mannosyltransferase activity in calf pancreas microsomes. Formation of ¹⁴C-labeled lipid-linked
808 oligosaccharides from GDP-D-[¹⁴C]mannose and pancreatic dolichyl beta-D-[¹⁴C]mannopyranosyl
809 phosphate. *J Biol Chem* 252, 224-234.

810 Laqueyrie, A., Militzer, P., Romain, F., Eiglmeier, K., Cole, S., and Marchal, G. (1995). Cloning,
811 sequencing, and expression of the *apa* gene coding for the *Mycobacterium tuberculosis* 45/47-
812 kilodalton secreted antigen complex. *Infect Immun* 63, 4003-4010.

813 Larsen, I. S. B., Narimatsu, Y., Joshi, H. J., Siukstaite, L., Harrison, O. J., Brasch, J., Goodman, K. M.,
814 Hansen, L., Shapiro, L., Honig, B., Vakhrushev, S. Y., Clausen, H., and Halim, A. (2017). Discovery of an
815 O-mannosylation pathway selectively serving cadherins and protocadherins. *Proc Natl Acad Sci U S A*
816 114, 11163-11168.

817 Larsen, I. S. B., Povolo, L., Zhou, L., Tian, W., Mygind, K. J., Hintze, J., Jiang, C., Hartill, V., Prescott, K.,
818 Johnson, C. A., Mullegama, S. V., McConkie-Rosell, A., McDonald, M., Hansen, L., Vakhrushev, S. Y.,
819 Schjoldager, K. T., Clausen, H., Worzfeld, T., Joshi, H. J., and Halim, A. (2023). The SHDRA syndrome-
820 associated gene TMEM260 encodes a protein-specific O-mannosyltransferase. *Proc Natl Acad Sci U S*
821 *A* 120, e2302584120.

822 Lee, M. H., and Hatfull, G. F. (1993). *Mycobacteriophage* L5 integrase-mediated site-specific integration
823 *in vitro*. *J Bacteriol* 175, 6836-6841.

824 Liu, C. F., Tonini, L., Malaga, W., Beau, M., Stella, A., Bouyssie, D., Jackson, M. C., Nigou, J., Puzo, G.,
825 Guilhot, C., Bulet-Schiltz, O., and Riviere, M. (2013). Bacterial protein-O-mannosylating enzyme is
826 crucial for virulence of *Mycobacterium tuberculosis*. *Proc Natl Acad Sci U S A* 110, 6560-6565.

827 Loibl, M., Wunderle, L., Hutzler, J., Schulz, B. L., Aebi, M., and Strahl, S. (2014). Protein O-
828 mannosyltransferases associate with the translocon to modify translocating polypeptide chains. *J Biol*
829 *Chem* 289, 8599-8611.

830 Malaga, W., Perez, E., and Guilhot, C. (2003). Production of unmarked mutations in mycobacteria using
831 site-specific recombination. *FEMS Microbiol Lett* 219, 261-268.

832 Many, H., Chiba, A., Yoshida, A., Wang, X., Chiba, Y., Jigami, Y., Margolis, R. U., and Endo, T. (2004).
833 Demonstration of mammalian protein O-mannosyltransferase activity: coexpression of POMT1 and
834 POMT2 required for enzymatic activity. *Proc Natl Acad Sci U S A* 101, 500-505.

835 Mehaffy, C., Belisle, J. T., and Dobos, K. M. (2019). *Mycobacteria* and their sweet proteins: An overview
836 of protein glycosylation and lipoglycosylation in *M. tuberculosis*. *Tuberculosis (Edinb)* 115, 1-13.

837 Ng, B. G., and Freeze, H. H. (2018). Perspectives on Glycosylation and Its Congenital Disorders. *Trends*
838 *Genet* 34, 466-476.

839 Orchard, M. G., Neuss, J. C., Galley, C. M., Carr, A., Porter, D. W., Smith, P., Scopes, D. I., Haydon, D.,
840 Vousden, K., Stubberfield, C. R., Young, K., and Page, M. (2004). Rhodanine-3-acetic acid derivatives as
841 inhibitors of fungal protein mannosyl transferase 1 (PMT1). *Bioorg Med Chem Lett* 14, 3975-3978.

842 Parra, J., Marcoux, J., Poncin, I., Canaan, S., Herrmann, J. L., Nigou, J., Burlet-Schiltz, O., and Riviere, M.
843 (2017). Scrutiny of *Mycobacterium tuberculosis* 19 kDa antigen proteoforms provides new insights in
844 the lipoglycoprotein biogenesis paradigm. *Sci Rep* 7, 43682.

845 Petrou, V. I., Herrera, C. M., Schultz, K. M., Clarke, O. B., Vendome, J., Tomasek, D., Banerjee, S.,
846 Rajashankar, K. R., Belcher Dufrisne, M., Kloss, B., Kloppmann, E., Rost, B., Klug, C. S., Trent, M. S.,
847 Shapiro, L., and Mancina, F. (2016). Structures of aminoarabinose transferase ArnT suggest a molecular
848 basis for lipid A glycosylation. *Science* 351, 608-612.

849 Pitarque, S., Herrmann, J. L., Duteyrat, J. L., Jackson, M., Stewart, G. R., Lecointe, F., Payre, B., Schwartz,
850 O., Young, D. B., Marchal, G., Lagrange, P. H., Puzo, G., Gicquel, B., Nigou, J., and Neyrolles, O. (2005).
851 Deciphering the molecular bases of *Mycobacterium tuberculosis* binding to the lectin DC-SIGN reveals
852 an underestimated complexity. *Biochem J* 392, 615-624.

853 Puschnik, A. S., Marceau, C. D., Ooi, Y. S., Majzoub, K., Rinis, N., Contessa, J. N., and Carette, J. E. (2017).
854 A Small-Molecule Oligosaccharyltransferase Inhibitor with Pan-flaviviral Activity. *Cell Rep* 21, 3032-
855 3039.

856 Ragas, A., Roussel, L., Puzo, G., and Riviere, M. (2007). The *Mycobacterium tuberculosis* cell-surface
857 glycoprotein apa as a potential adhesin to colonize target cells via the innate immune system
858 pulmonary C-type lectin surfactant protein A. *J Biol Chem* 282, 5133-5142.

859 RCoreTeam (2022).R: A language and environment for statistical computing.: R Foundation for
860 Statistical Computing, Vienna, Austria.

861 Rex, J. H., Fernandez Lynch, H., Cohen, I. G., Darrow, J. J., and Outterson, K. (2019). Designing
862 development programs for non-traditional antibacterial agents. *Nat Commun* 10, 3416.

863 Richards, J. B., and Hemming, F. W. (1972). The transfer of mannose from guanosine diphosphate
864 mannose to dolichol phosphate and protein by pig liver endoplasmic reticulum. *Biochem J* 130, 77-93.

865 Sartain, M. J., and Belisle, J. T. (2009). N-Terminal clustering of the O-glycosylation sites in the
866 *Mycobacterium tuberculosis* lipoprotein SodC. *Glycobiology* 19, 38-51.

867 Schnappinger, D., Ehrt, S., Voskuil, M. I., Liu, Y., Mangan, J. A., Monahan, I. M., Dolganov, G., Efron, B.,
868 Butcher, P. D., Nathan, C., and Schoolnik, G. K. (2003). Transcriptional Adaptation of *Mycobacterium*
869 *tuberculosis* within Macrophages: Insights into the Phagosomal Environment. *J Exp Med* 198, 693-704.

870 Schultz, J. C., and Takayama, K. (1975). The role of mannosylphosphorylpolyisoprenol in glycoprotein
871 biosynthesis in *Mycobacterium smegmatis*. *Biochim Biophys Acta* 381, 175-184.

872 Sjodt, M., Brock, K., Dobihal, G., Rohs, P. D. A., Green, A. G., Hopf, T. A., Meeske, A. J., Srisuknimit, V.,
873 Kahne, D., Walker, S., Marks, D. S., Bernhardt, T. G., Rudner, D. Z., and Kruse, A. C. (2018). Structure of
874 the peptidoglycan polymerase RodA resolved by evolutionary coupling analysis. *Nature* 556, 118-121.

875 Smith, G. T., Sweredoski, M. J., and Hess, S. (2014). O-linked glycosylation sites profiling in
876 *Mycobacterium tuberculosis* culture filtrate proteins. *J Proteomics* 97, 296-306.

877 Spratt, J. M., Britton, W. J., and Triccas, J. A. (2003). Identification of strong promoter elements of
878 *Mycobacterium smegmatis* and their utility for foreign gene expression in mycobacteria. *FEMS*
879 *Microbiol Lett* 224, 139-142.

880 Stewart, G. R., Wilkinson, K. A., Newton, S. A., Sullivan, S. A., Neyrolles, O., Wain, J. R., Patel, J., Pool,
881 K. L., Young, D. B., and Wilkinson, R. J. (2005). Effect of deletion or overexpression of the 19-kilodalton
882 lipoprotein Rv3763 on the innate response to *Mycobacterium tuberculosis*. *Infect Immun* 73, 6831-
883 6837.

884 Stover, C. K., de la Cruz, V. F., Fuerst, T. R., Burlein, J. E., Benson, L. A., Bennett, L. T., Bansal, G. P.,
885 Young, J. F., Lee, M. H., Hatfull, G. F., and et al. (1991). New use of BCG for recombinant vaccines.
886 *Nature* 351, 456-460.

887 Szafranski-Schneider, E., Swidergall, M., Cottier, F., Tielker, D., Roman, E., Pla, J., and Ernst, J. F. (2012).
888 Msb2 shedding protects *Candida albicans* against antimicrobial peptides. *PLoS Pathog* 8, e1002501.

889 Theuretzbacher, U., and Piddock, L. J. V. (2019). Non-traditional Antibacterial Therapeutic Options and
890 Challenges. *Cell Host Microbe* 26, 61-72.

891 Tonini, L., Sadet, B., Stella, A., Bouyssié, D., Nigou, J., Burlet-Schiltz, O., and Riviere, M. (2020). Potential
892 Plasticity of the Mannoprotein Repertoire Associated to *Mycobacterium tuberculosis* Virulence
893 Unveiled by Mass Spectrometry-Based Glycoproteomics. *Molecules* 25.

894 Torrelles, J. B., and Schlesinger, L. S. (2010). Diversity in *Mycobacterium tuberculosis* mannosylated
895 cell wall determinants impacts adaptation to the host. *Tuberculosis (Edinb)* 90, 84-93.

896 van Els, C. A., Corbiere, V., Smits, K., van Gaans-van den Brink, J. A., Poelen, M. C., Mascart, F., Meiring,
897 H. D., and Locht, C. (2014). Toward Understanding the Essence of Post-Translational Modifications for
898 the *Mycobacterium tuberculosis* Immunoproteome. *Front Immunol* 5, 361.

899 VanderVen, B. C., Harder, J. D., Crick, D. C., and Belisle, J. T. (2005). Export-mediated assembly of
900 mycobacterial glycoproteins parallels eukaryotic pathways. *Science* 309, 941-943.

901 Verma, A. K., Raizada, M. K., and Schutzbach, J. S. (1977). Formation of alpha-1,2-mannosyl-mannose
902 by an enzyme preparation from rabbit liver. *J Biol Chem* 252, 7235-7242.

903 WHO (2021). Global Tuberculosis Report pp. 1–43

904 Wickham, H., Averick, M., J., B., Chang, W., McGowan, L. D., François, R., Grolmund, G., A., H., Henry,
905 L., Hester, J., Kuhn, M., Pedersen, T. L., Miller, E., Bache, S. M., Müller, K., Ooms, J., Robinson, D., Seidel,
906 D. P., Spinu, V., Takahashi, K., Vaughan, D., Wilke, C., Woo, K., and Yutani, H. (2019). Welcome to the
907 tidyverse. *Journal of Open Source Software* 4(43).

908 Wiker, H. G. (2009). MPB70 and MPB83--major antigens of *Mycobacterium bovis*. *Scand J Immunol* 69,
909 492-499.

910 Wild, R., Kowal, J., Eyring, J., Ngwa, E. M., Aebi, M., and Locher, K. P. (2018). Structure of the yeast
911 oligosaccharyltransferase complex gives insight into eukaryotic N-glycosylation. *Science* 359, 545-550.

912 Yadav, U., and Khan, M. A. (2018). Targeting the GPI biosynthetic pathway. *Pathog Glob Health* 112,
913 115-122.

914 Zhang, L., Zhao, Y., Gao, Y., Wu, L., Gao, R., Zhang, Q., Wang, Y., Wu, C., Wu, F., Gurcha, S. S., Veerapen,
915 N., Batt, S. M., Zhao, W., Qin, L., Yang, X., Wang, M., Zhu, Y., Zhang, B., Bi, L., Zhang, X., Yang, H., Guddat,
916 L. W., Xu, W., Wang, Q., Li, J., Besra, G. S., and Rao, Z. (2020). Structures of cell wall
917 arabinosyltransferases with the anti-tuberculosis drug ethambutol. *Science* 368, 1211-1219.

918